Photocopy and Use Authorization

In presenting this dissertation in partial fulfillment of the requirements for an advanced degree at Idaho State University, I agree that the Library shall make it freely available for inspection. I further state that permission for extensive copying of my thesis for scholarly purposes may be granted by the Dean of the Graduate School, Dean of my academic division, or by the University Librarian. It is understood that any copying or publication of this thesis for financial gain shall not be allowed without my written permission.

Signature _____

Date_____

A PBPK Based Modeling Approach for Molybdenum

by

Kishor Paudel

A dissertation

submitted in partial fulfillment

of the requirements for the degree of

Doctor of Philosophy in the Department of Nuclear Engineering

Idaho State University

Summer 2021

To the Graduate Faculty:

The members of the committee appointed to examine the dissertation of Kishor Paudel find it satisfactory and recommend that it be accepted.

_____

Richard R. Brey, Ph.D.

Major Advisor

_____

Thomas F. Gesell, Ph.D.

Committee Member

_____

Chad L. Pope, Ph.D.

Committee Member

_____

Scott C. Miller, Ph.D.

Committee Member

_____

DeWayne R. Derryberry, Ph.D.

Graduate Faculty Representative

Dedication, and Acknowledgments

I dedicate my dissertation to my family in Nepal, and my wife Sujata Tiwari. I also would like to dedicate my dissertation to our newly born daughter, Aizel Paudel.

I would like to thank my committee members who were extremely generous with their time, and expertise in support of my research efforts. My research advisor, Dr. Richard Brey, deserves special recognition for his tireless efforts to support my research. I also would like to thank my friend Dr. Mark T. Williams for his intellectual input.

TABLE OF CONTENTS

LIST OF FIGURES

LIST OF TABLES

A PBPK Based Modeling Approach for Molybdenum

Dissertation Abstract -- Idaho State University (2021)

Molybdenum (Mo) is an essential trace element for humans and animals and is required for the function of four enzymes found in humans. Molybdenum-99 is among the most important radionuclides in radiological protection because it decays with a 66-hour half-life by isobaric decay emitting a negatron. But, more importantly it is the decay precursor of metastable Technicium-99 which arguably is among the most important radionuclides used for diagnostic nuclear medicine. Molybdenum-99 has the potential to be released in the environment in large amounts as a result of accidents in nuclear power plants, nuclear medical installations or in transportation accidents, consequently it is considered a potential occupational or public health concern. The goal of this study was to develop a physiologically based methodology for describing the metabolic behavior of molybdenum within the human body from occupational, environmental, and medical exposure. Current internal dosimetry biokinetic models describe the distribution, clearance, and organ retention of internalized radioactive materials. These models are most frequently developed using bioassay data. Parameter are added to these models to enhance fits to measured bioassay parameters. However, physiologically based pharmacokinetic (PBPK) modeling was used in this study to understand the behavior of molybdenum within the human body. PBPK models seek to fundamentally measure and understand organ kinetics. This approach could enhance understanding of organ retention and excretion and ultimately improve the predictive capability of current internal dosimetry biokinetic models. The International Commission on Radiological Protection's (ICRP) molybdenum model and the Giussani molybdenum model were reconstructed in the SAAM II software. Eight and six compartmental PBPK models (model-A, and model-B) were proposed in this project. To test the validity of the purposed models, model-A and model-B

were developed in a format compatible with the SAAM II software. The Akaike Information Criterion (AIC) statistic was used to quantitatively evaluate the quality of the models. The AIC values were obtained from the software and were used to find the best fits. Based on the AIC values, it was concluded that the ICRP model was the least favorable model, and that model-A was more favorable model.

Key Words: Molybdenum, Compartmental model, Internal Dosimetry, PBPK, biokinetic model, AIC, SAAM II.

CHAPTER 1. INTRODUCTION

1.1 Background

Molybdenum (Mo) is an essential trace element for humans and animals and is required for the function of four enzymes found in humans. There are 11 isotopes of molybdenum. Molybdenum-99 is the most important radioisotopes in radiological protection because it decays with a 66-hour half-life by undergoing an isobaric transition emitting a negatron. As such, about 88% of the decays produce technicium-99m, which has important and widespread uses in nuclear medicine (^{99m}Tc, has a 6-hour half-life). It is also important in radiological protection because it is so frequently used in a large quantity. Elemental molybdenum may be present in industry in a variety of chemical forms, including oxides, halides, sulfides, nitrates, and ammonium molybdate. Molybdenum-99 has an ability to be released in the environment in large amounts as a result of accidents in nuclear power plants or nuclear medical installations or in transportation accidents. Consequently, it may be an occupational or public health concern.

1.1.1 Physiology of Molybdenum

The kidneys are the main regulators of molybdenum levels in the human body and are responsible for its excretion via the urinary pathway. Understanding the metabolic behavior of molybdenum inside the body is important in the construction of models that can be used to predict its behavior and ultimately its chemical, and radiation toxicity.

1.2 Objective

The objective of this research was to develop a metabolically based model using the PBPK modeling approach for molybdenum to better define and understand the physiological relevance of kidney transfer rates in humans. The objective of creating an approved PBPK model is that it ideally would provide increased accuracy of the physiological basis for kinetic transfer rates.

1.3 Hypothesis Testing

Two hypotheses will be tested in this project using the excretion data described in section 3.1. Decisions will be made by comparing proposed models, namely model-A, and model-B (described in section 3.4), using the Akaike Information Criterion (AIC) values (described in section 2.7.1).

The AIC is a way of selecting a model from a set of models. The AIC compares the goodness of fit of a set of statistical models to each other. The AIC assigns a score to each model, and the lowest score is considered the best fit. A SAMM II software (described in section 3.5) was used to construct the before mentioned models. The AIC values were obtained from the software and were used to find the best fits. Two hypotheses along with the decision rules which will be tested in this project are listed below[1].

$H_{0,1}$: Most of the molybdenum excretion in the kidney is predominantly a function of glomerular filtration.

$H_{A,1}$: Most of the molybdenum excretion in the kidney is not predominantly a function of glomerular filtration.

$H_{0,2}$: Molybdenum excretion in the kidney follows linear kinetics.

$H_{A,2}$: Molybdenum excretion in the kidney does not follows linear kinetics.

Decision rule: The model associated with the lower AIC score is considered more probable.

[1] Excretion data were used in this project.

CHAPTER 2. LITERATURE REVIEW

2.1 What is Molybdenum?

Molybdenum is a group six transition metal in the periodic table. Molybdenum does not naturally occur in the native elemental state, but is obtained from the ores molybdenite, wulfenite, ferrimolybdate and jordicite (Gharehbaghi et al., 2011). Molybdenum is an essential trace element for humans and animals, but too much of it is toxic. The lethal dose for repeated oral administration is 60 to 333 mg kg^{-1} day^{-1} for soluble molybdenum compounds administered to rats, mouse, guinea pigs, and rabbits (Fairhall et al., 1945 and Arrington and Davis 1953). Molybdenum is a structural constituent of molybdoprotein, a cofactor synthesized by the body and required for the functions of a few enzymes (NIH 2020). It was established that the daily molybdenum requirement of human is approximately 25.0 μg or possibly less while an intake of 150 μg per kg body weight might be toxic (Gharehbaghi et al., 2011).

2.1.1 Brief History of Molybdenum

Molybdenum was discovered by Carl Welhelm Scheele, a Swedish chemist, in 1778 in mineral known as MoS_2 which was confused as a lead compound. Molybdenum was isolated by Peter Jacob Hjelm in 1781. Molybdenum today is mostly obtained from molybdenite. Molybdenum is also obtained from byproducts of mining and processing tungsten and copper. Molybdenum remained mainly a laboratory curiosity until the 19th century, when technologies for the extraction of commercial quantities became practical. The French company Schneider & Co. first used molybdenum as an alloying element in armor plate steel since 1981 (IMOA 2020).

2.1.2 Chemical and Physical Properties

There are 11 isotopes of molybdenum. Its radioisotope molybdenum-99 may be released in significant amounts as a result of accidents in nuclear power plants, nuclear medical installations

or in transportation accidents, therefore it is considered a potential occupational or public health concern. The activity of molybdenum-99 released after the Chernobyl nuclear disaster for instance, was greater than 7.2 x 10^{16} Bq (Mclaughlin et. al., 2012).

The melting and boiling point of molybdenum are 2,610, and 4,825 degrees Celsius, respectively (Lenntech 2014). Molybdenum has one of the highest melting points among all pure elements. Atomic weight and density for element molybdenum are 95.9 g, and 10.2 g/cm^3, respectively. As such, the vapor pressure of molybdenum is 7.5 x 10^{-3} torr at 2469 °C (Speight 2017). Molybdenum metal is a silvery white; it is a very hard transition metal but is softer and more ductile than tungsten. Molybdenum reacts slowly with acids. Seven naturally occurring isotopes of molybdenum are: molybdenum-92, molybdenum-94, molybdenum-95, molybdenum-96, molybdenum-97, molybdenum-98, and molybdenum-100 (Lenntech 2014). Molybdenum has a +4 or +6 charge (Mo^{4+} and Mo^{6+}) when in the human body. Where it typically is bound to sulphur or oxygen. However, in general, oxidation states of molybdenum-99 are +2, +3, +4, and +6 (Nordberg et al., 2007).

Molybdenum is the 25th most abundant element in sea water at an average concentration of 100 nano-molar (nM). Its concentration in continental water is much lower around 5 nM. Furthermore, in the geosphere, molybdenum concentration is 3 mg kg^{-1}, but this increases up to 300 mg kg^{-1} when the organic matter is high (Maret and Wedd 2014).

Technetium-99m (^{99m}Tc) used in nuclear medicine today is produced by radioactive decay of ^{99}Mo (Figure 1). Molybdeuum-99 decays with about a 66-hour half-life by isobaric transition producing a negatron. About 80% of the decays produce ^{99m}Tc with a 6-hour half-life as shown in Figure 1. As such, ^{99m}Tc decays to ^{99}Tc via isomeric transition and releases gamma rays and low energy electrons (Washington State Department of Health, 2002). Molybdenum-99 can be

produced by a number of processes using nuclear reactors or accelerators. The primary production method is fission of Uranium-235(^{235}U) in the production reactors with the yield of 80-85% (NCBI 2016).

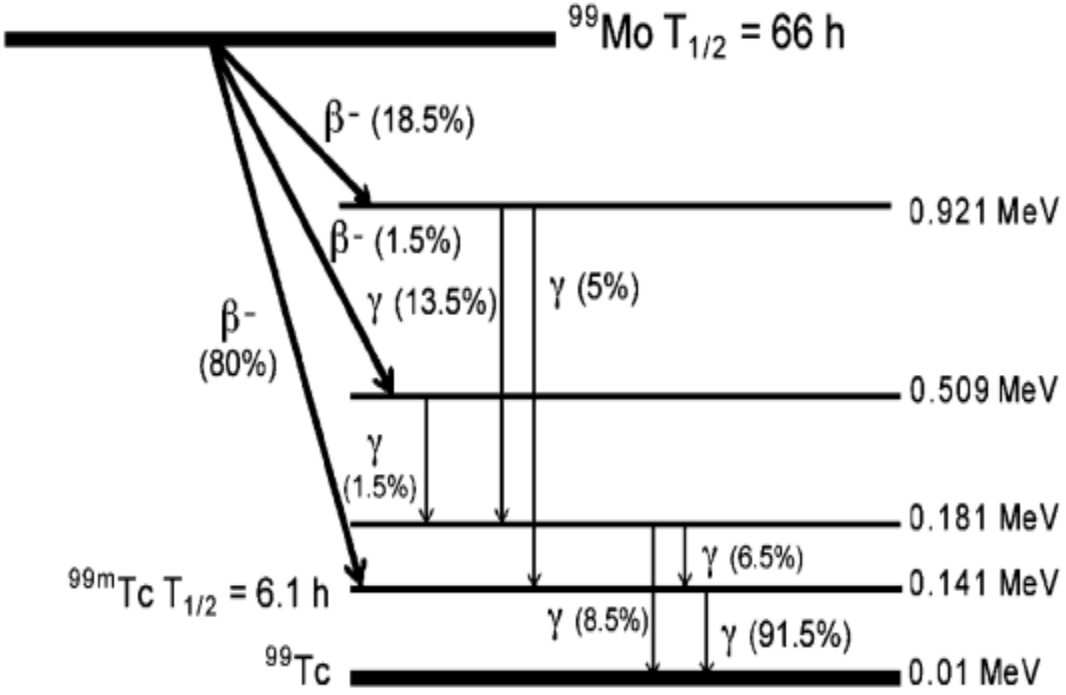

Figure 1. Decay scheme of ^{99}Mo and ^{99m}Tc (adopted from Pillai et al., 2012)

2.1.3 Applications of Molybdenum

2.1.3.1 Industrial Applications

Molybdenum is a valuable alloying agent because it helps in hardening and toughness of quenched and tempered steel. It also increases the strength of steel at high temperature. Molybdenum has various industrial applications, such as: alloying agent in steel and cast iron, pigment for printing ink, catalysts, and solid lubricants. Molybdenum powders are used in circuit inks for circuit boards, and in microwaves devices and as heat sink for solid state devices (Voropanova and Barvinyuk 2004).

2.1.3.2 Clinical Applications

Molybdenum has been clinically used to treat Wilson's disease (Brewer et al., 2009). Wilson's disease is a genetic disorder in which excess copper builds up in the body resulting in liver damage, neurological complications, and brain damage (Mayo Clinic 2020). Molybdenum as tetrathiomolybdate can form a strong complex with copper and protein (Brewer et al., 2009). Tetrathiomolybdate given with food forms complexes with dietary copper and protein and prevents copper absorption. Tetrathiomolybdate given without food is absorbed into the bloodstream and forms complexes with circulating copper and albumen, preventing the copper from accumulating in cells and causing toxicity (Brewer et al., 2009).

Molybdenum biokinetics is also of interest in radiological protection because of the frequent use of molybdenum-99 in ^{99m}Tc generators in medical applications (Giussani et al., 2006). Metastable technetium-99 is used in approximately 80 percent of all nuclear medical procedures worldwide each year. Metastable ^{99}Tc is used primarily as a medical diagnostic tool, and it can be found as a component of industrials and institutional wastes from hospitals and research laboratories. Furthermore, ^{99m}Tc is used in medical diagnostics in brain, bone, liver, spleen, kidney, and thyroid scanning and for blood flow studies (EPA 2002). ^{99m}Tc has a short, six-hour half-life and does not remain in the body or the environment for long period of the time (EPA 2017).

Current global demand for molybdenum-99 is estimated to be about 9,000 6-day Curies (Ci) per week, about half of which is consumed in the United States (NCBI 2016). Over 95% of global supply of molybdenum-99 is supplied from the SHINE, a medical isotope producer, from processing facilities located in the U.S., Australia, Europe, and South Africa (SHINE 2021).

2.1.4 Food Sources

Molybdenum is a component of certain mammalian metalloflavoproteins. Plants need Mo for fixing of atmospheric nitrogen by bacteria at the start of protein synthesis. So, molybdenum is ubiquitous in food (European Commission, 2000). The amount of molybdenum in food depends on the amount of molybdenum in soil and the water used for irrigation (NIH 2020). Legumes are the richest sources of dietary molybdenum. Other foods with high molybdenum content include whole grains, nuts, beef liver, cereal grains, leafy vegetables, milk, and cheese (NIH 2020). Fruits, root vegetables, and meat are poor sources of molybdenum (NIH 2020 and European Commission 2000).

2.1.5 Biological use of Molybdenum in Human Body

Four human enzymes that require molybdenum have been identified to date: sulfite oxidase, xanthine oxidase, aldehyde oxidase, and mitochondrial amidoxime-reducing component (mARC) (Novonty and Peterson 2018). Sulfite oxidase, an enzyme found in mitochondria, catalyzes oxidation of sulfite to sulfate, which is the final step in oxidation of sulfur amino acids. Xanthine oxidase converts hypoxanthine to xanthine, and further converts xanthine to uric acid. Likewise, it also prevents hypoxanthine, from leading to DNA mutations if paired with cytosine in place of thymine. Aldehyde oxidase found in the liver is an important enzyme in phase 1 drug metabolism. Enzyme mARC works in concert with cytochrome b5 type B and NAD (H) cytochrome b5 reductase to reduce a variety of N-hydroxylated substrates, however, the physiologic significance is still unclear (Novonty and Peterson 2018). Out of four enzymes, only sulfite oxidase is known to be indispensable for human beings (Rajagopalan 1987). These enzymes have a common essential cofactor, molybdoprotein (Mills and Davis 1987). Furthermore, Mo is involved in the metabolism of purines, pyridines, quinolines, sulfite, and bisulfite (Desai 2000).

2.1.6 How the Public might be Exposed to Molybdenum?

One may wonder how public might be exposed to molybdenum. Following are a few possible ways that people might get exposed to molybdenum (Department of State Health Services, Texas, 2012).

a. Molybdenum is ubiquitous in nature; therefore, the general public can be exposed to small amounts of Mo in the air or eating food or drinking water.
b. The public may come into contact with molybdenum containing dust carried on the clothes of workers occupationally exposed to Mo.
c. An occupational worker using an electroplating process may be exposed to dusts and fumes containing molybdenum.

2.2 Molybdenum Metabolism

2.2.1 Molybdenum Absorption

2.2.1.1 Inhalation

Few published sources of data are available on the absorption of molybdenum after inhalation in humans following accidental intakes or from experimental studies in animals. Guinea pigs showed no noticeable absorption after exposure through inhalation to 285 mg/m^3 of Mo as molybdenum disulfide (Nordberg et al., 2007). The ICRP 30, part I 1979, has assigned all compounds of molybdenum (except oxides, hydroxides, and MoS_2 with inhalation class Y) to inhalation class D with an absorption coefficient of 0.8. The protective action criteria (PAC) of molybdenum for PAC-1, PAC-2. PAC-3 are 30, 330, and 2000 mg/m^3, respectively[2].

[2] https://edms.energy.gov/pac/Search/Reports/1996

Some of the inhalation health effects of molybdenum are nose, and throat irritation with coughing and wheezing (NJ Health 2011). Occupational exposures might occur through inhalation, and dermal contact at workplaces where molybdenum compounds are used or manufactured.

2.2.1.2 Ingestion

Water-soluble molybdenum compounds are readily absorbed when ingested. The rate of absorption depends on the chemical form and the animal species. Molybdenum absorption varies in animals between 75 to 97% (Table 1). Table 1 shows that in human absorption of molybdenum via the digestive tract after oral intake has been found to be in the range 28 to 77% (Vyskocil and Viau 1999). Low amounts of molybdenum are absorbed by active transport, but higher amounts only require simple diffusion. It is transported into the blood by either albumin or alpha-2 macroglobulin (Preston 2014).

Table 1. Summary of Mo Absorption in Animals and Humans (Vvskocil and Viau 1999)

Species	Form	Route	Absorption (%)
Rat	^{99}Mo (molybdate)	Oral	97
Rat	MoS_2	Oral-diet	0
Guinea Pig	MoO_3	Oral	88
Pig	$(NH_4)_2MoO_4$	Oral	75
Human	Unknown	Oral-diet	28,52
Human	Unknown	Oral-diet	77
Human	Unknown	Oral-diet	28-62

Molybdenum once absorbed, via inhalation or ingestion, appears rapidly in the blood and most organs. Blood molybdenum concentrations for humans are normally from 5 µg/l to 400 µg/l (Allaway et. al., 1968). The concentration of molybdenum occurs in kidneys, liver, and bone (Nordberg et al., 2007). The key molybdenum excretory pathway is urine via the kidneys, which is very rapid (Nordberg et al., 2007). The biological half-life ranges from a few hours to few days. Turnover is much more rapid when molybdenum intake is high and vice-versa (Nordberg et al.,

2007). Molybdenum is easily absorbed in the stomach and upper intestine and is attached to proteins for transport in blood, for tissue storage and for use as an enzyme cofactor (Thompson and Turnlund 1996).

The amount of molybdenum absorption not only depends on the level of molybdenum, but also on the level of dietary copper and sulfate (Nordberg et al., 2007). Copper forms insoluble copper thiomolybdate in the digestive tract (Sardesai 1993). Higher amount of inorganic sulfate (300 to 400 PPM) might block the transport of molybdenum through cell membranes, and as a result reduces the intestinal absorption and renal tubular reabsorption (Mills and Brenner 1980).

2.2.2 Molybdenum Distribution

Molybdenum in the human blood is bound in the form of molybdate. It is specifically bound to α_2-macroglobulin (mass: 725,000 kilodalton(kDa)), and in erythrocytes to protein of the erythrocyte membrane, mainly spectrin (mass: 230 kDa) (Kselikova et al, 1980). Molybdenum concentration in the blood of humans increase as its dietary intake increases. Turnlund and Keys observed in humans that molybdenum concentration increased from 4 to 44 nmol/l in plasma when intake increased from 22 to 1,400 µg/day (Turnlund and Keyes 2004). Blood concentrations of molybdenum rise after meals, this peaks after an hour after meals, and then returns to basal levels. Study performed by Turnlund et al., 1995 observed that when the low diet-molybdenum (22 µg/day) was fed to humans, 41% of the total molybdenum was eliminated via feces and 59% via urine. As such, when higher amounts of molybdenum (1,490 µg/day) were fed to humans, 6% of the total molybdenum ingested was excreted via feces and 94% excreted via urine.

Studies performed by Giussani et al., 2006, and Giussani et al., 2007 on intestinal absorption of molybdenum in humans, and modeling urinary excretion of molybdenum after oral and intravenous administration of stable tracers are of immense interest. The findings were thought

to be important because these experiments found that molybdenum excretion mostly occur via the kidneys rather than the liver.

2.2.2.1 Intestinal Absorption of Molybdenum in Humans (Giussani et al., 2006)

Isotropic solutions were prepared using metal powders enriched in ^{95}Mo, and ^{96}Mo and were injected intravenously in a few human volunteers to study the intestinal absorption of molybdenum by Giussani et al., 2006. Molybdenum absorption into the systematic circulation is nearly complete when provided in liquids solutions, but this is reduced by a factor of 2 when molybdenum in provided in solid foodstuffs in a bound form. No discrepancy is observed between the results from male and female volunteers. The reduced absorption for administration with solid food is thought to be related to a lower bioavailability of molybdenum due to interactions with components of foods. The administration of high amount of molybdenum in liquid forms (greater than 40 g per kg body weight), the fraction absorbed decreases. Furthermore, Giussani et al., 2006 also observed that administration of black tea dramatically affected the Mo absorption, reducing it at least by a factor of 5. The effects of black tea are probably due to the presence of phenolic compounds (tannins), a powerful inhibitor of gut uptake (Disler et al., 1975). Giussani et al., 2006 also observed that absorption of molybdenum from other sites than the upper part of the alimentary tract seems to be negligible. The International Commission on Radiological Protection's (ICRP) model considers an absorbed fraction of 0.8 for workers and a value of 1 for adult members of the public as a conservative value.

Measurements of the molybdenum tracers' concentration in blood plasma show that elimination from the blood plasma proceeds rapidly and can be explained by using a bi-exponential function with characteristic times of approximately 0.3 hour and 3.5 hour, respectively (Giussani

et al., 2006). The ICRP model considers a slower mono-exponential clearance with a 6-hour half-life.

2.2.2.2 Urinary Excretion of Molybdenum (Giussani et al., 2007)

Isotropic solutions were prepared using metal powders enriched in ^{95}Mo, and ^{96}Mo and were injected intravenously in a few human volunteers to study the urinary excretion of molybdenum by Giussani et al., 2007. Urinary excretion of incorporated molybdenum is very rapid. Most of the urinary excretion takes place in the first few hours after incorporation and at 48-hour excretion is negligible. As such, the percentage excreted molybdenum increases with increasing amount of circulating molybdenum. The cumulated 48-hour excretion of molybdenum after intravenous injection amounts to 35% by administration of 100 µg Mo and increases up to 72% if an extra oral dose (up to 5 mg Mo) is simultaneously administered. Furthermore, the excretion of already stored systematic molybdenum is enhanced. This fact suggests a mobilization of stored molybdenum because of the introduction into the system of additional molybdenum. The ICRP model describes a slower elimination via the renal pathway, with less than 7% eliminated over 48 hours, and 14% over one week.

2.2.3 Excretion

The amount of urinary excretion of molybdenum depends on the amount and modality of intake. The exposure routes can be via inhalation, ingestion, skin, and or eye contact (CDC 2021).

2.2.4 Biological Half-Life of Molybdenum

The excretion of molybdenum and its rapid clearance from the liver, kidney, spleen, testis, and hard tissues (living, mineralized tissues that poses a high degree of hardness) in animals show that biological half-life for the major fraction of absorbed molybdenum from the pulmonary system, and the GI tract must be in the range of hours and extending up to a maximum of 1 day in

animals (Nordberg et al., 2007). The half-life in healthy adults is influenced by dietary intake and is much shorter when intake is high than when it is low. Half-life of plasma clearance in humans were estimated to be between 4 and 70 minutes for fast component and between 2 and 30 hours for a slow component. Residence time for molybdenum in the GI tract is estimated at 1.7 days. Residence time for plasma molybdenum is 22 min, whereas for slow turnover tissue (possibly hepatic) retention time is 58 days (Thompson and Turnlund 1996). Furthermore, Thompson and Turnlund found that when a small dose of ^{97}Mo, and ^{100}Mo were injected intravenously, 34% of the dose were excreted in the urine within 1 day, and 60% were excreted when large dose is ejected within 1 day (Thompson and Turnlund 1996).

2.2.5 Molybdenum Deficiency

Most Americans appear to consume adequate amounts of molybdenum, and as a result molybdenum deficiency has not been reported. The only apparent documented case of dietary molybdenum deficiency was in a man with Crohn's disease and short-bowel syndrome who was receiving permanent parenteral nutrition and demonstrated of molybdenum deficiency (Abumrad 1984). As such, in people with a genetic mutation that prevents the synthesis of molybdoprotrein and sulfite oxidase might have molybdenum deficiency (NIH 2020).

2.2.6 Molybdenum Toxicity

The annual radiological limit on intake, from an oral ingestion of ^{99}Mo compounds except oxides, hydroxides, and molybdenum disulfide is 7.4 x 10^6 Bq. Moreover, derived air concentration[3] of ^{99}Mo compounds except oxides, hydroxides, and molybdenum disulfide is 3.7 x 10^{-3} Bq/mL. The American Conference of Governmental Industrial Hygienists (ACGIH)

[3] Source: Source: https://www.atsdr.cdc.gov/ToxProfiles/tp212-c7.pdf

recommended threshold limit value-time weighted average (TLV-TWA)[4] value for molybdenum (includes metal dust and the dioxide) is 10 mg/m^3.

Molybdenum chemical toxicity depends upon animal species and chemical form. Soluble molybdenum compounds are more toxic than insoluble ones. Mostly over exposure symptoms resemble those of copper deficiency, however, treatment with supplemental copper may reverse them. Symptoms may also be produced when dietary copper is normal, but molybdenum content is higher than normal (Vyskocil and Viau 1999). Rapid elimination of Mo from the bloodstream keeps blood concentration very low (~10 nmol/L). While in tissue Molybdenum concentration may range up to 10 µmol/L (Versieck et al., 1978).

The chemical molybdenum toxicity is little known in humans, so knowledge of molybdenum toxicity is based on experiments with animals. A low order of toxicity of molybdenum compounds has been observed in humans, however, it is not sufficient enough to calculate any dose effect relationship. Human lethal dose of molybdenum was unknown (Vyskocil and Viau 1999). However, the lethal dose for repeated oral administration is 60 to 333 mg/(kg–day) for soluble molybdenum compounds administered to rats, mouse, guinea pigs, and rabbits (Fairhall et al., 1945 and Arrington and Davis 1953). Histological examinations of animals after acute dose generally show damage to the liver, and kidney and sometimes to the adrenals and spleen (Vyskocil and Viau 1999). Higher levels of uric acid and gout-like symptoms have been reported among workers exposed to molybdenum in a copper-molybdenum plants and general population living in the areas with high molybdenum and copper contents in soils and vegetables (Walravens et al., 1979). Metallic molybdenum and sparingly soluble molybdenum trioxide might cause lung damage if inhaled. Pneumoconiosis has been reported in a few cases.

[4] Source: httpss://www.cdc.gov/niosh/pel88/7439-98.html

2.3 Molybdenum Cofactor

Molybdenum itself is catalytically inactive in biological systems until it is complexed by a special scaffold. One type of scaffold is the ubiquitous pterin-based molybdenum cofactor (Mendel 2013). To understand the Molybdenum cofactor, knowledge of an enzyme kinetics is essential.

2.3.1 Enzyme Kinetics

An enzyme is a protein with catalytic properties. As a catalyst, an enzyme lowers the energy of activation of a reaction, therefore increasing the rate of that reaction without affecting the position of equilibrium. The knowledge of the kinetics of an enzyme can provide the useful information about its catalytic mechanism, role in metabolism, factors that impact its activity, and mechanisms of inhibition. An enzymatic reaction is divided in to a two-step process (Equation 1): substrate (S) binding by enzyme (E) and formation of an enzyme-substrate (ES) complex, followed by an irreversible breakdown of the enzyme-substrate complex to free enzyme and product (P) (Marangoni 2003). The reversible part in Equation 1 has the reaction rate constant (RC) of k_{+1} to produce the ES complex with RC k_{+2} (not a reversible reaction). The rate of the reaction (V), which is the rate at which product is formed, is defined by Equation 2.

$$E + S \Leftrightarrow ES \Rightarrow P + E \qquad \text{Eq (1)}$$

$$V = d[P]/dt = k_{+2}[ES] \qquad \text{Eq (2)}$$

Where, the square brackets represent the molar concentration of the substrate specified within.

The Michaelis-Menten equilibrium model (Figure 2)[5] describes the action of enzymes mathematically. The maximal velocity (V_{max}) refers to the point at which the increase in the concentration of the substrate does not increase the rate of a reaction catalyzed by an enzyme. Moreover, the Michaelis constant (K_m) is the concentration of the substrate when half of the active

[5] Figure 2 adopted from https://microbenotes.com/the-michaelis-menten-model/

binding sites of an enzyme are occupied by the substrate. K_m constant helps to depict the affinity of an enzyme for their substrates. An enzyme with a high k_m has a low affinity for the substrate, and a higher concentration of the substance is needed for the enzyme to become saturated and vice-versa. The knowledge of V_{max} and K_m plays a key role to explaining how enzymes work and assist in the prediction of the behavior of enzymes in living organisms.

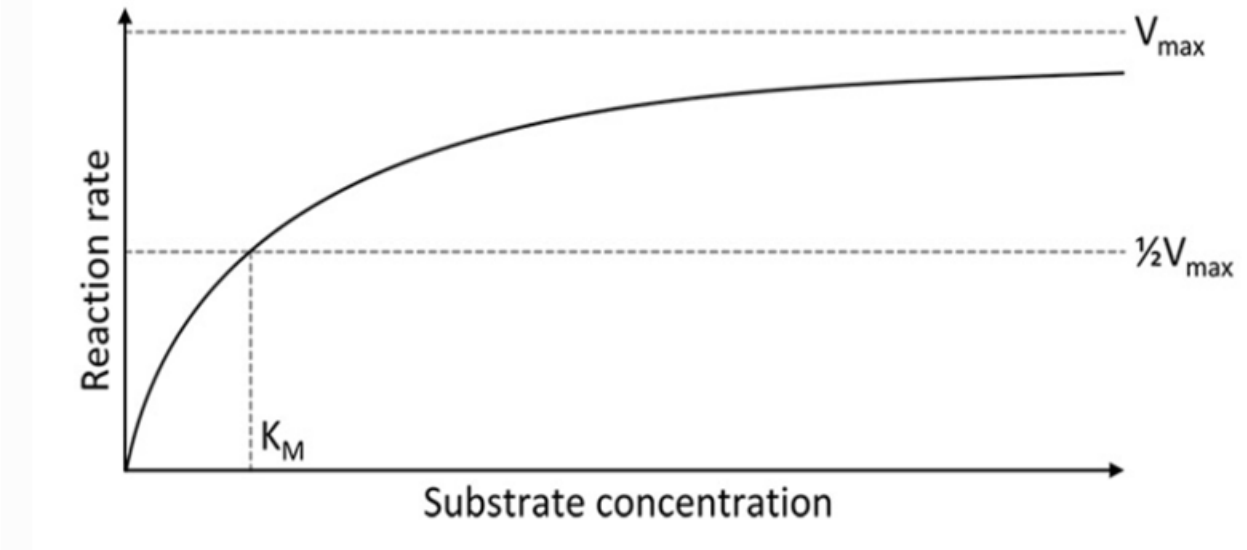

Figure 2. Michaelis-Menten Model (Kinetics)

2.3.2 What is Molybdenum Cofactor (Moco)?

Molybdenum is said to have a versatile redox chemistry that is used by the enzymes to catalyze diverse redox reactions. Molybdenum enzymes catalyze the transfer of an oxygen atom (derived from water) to or from a substrate (Mendel 2013). Each reaction (either reduction or oxidation) involves the transfer of two electrons eventually causing a change in the oxidation state of the Molybdenum atom in the substrate site from 4 to 6 or vice versa (Lobbi-Nivol and Leimkuhler 2013).

It appears that the metal is not directly attached to the catalytic site. Rather the molybdenum atom is complexed within a specific low molecular scaffold to fulfil its catalytic function. The resultant compound is a unique tricyclic pterin called molybdoprotein or metal-containing pterin

(MPT). Consequently, due to the combination of molybdenum with MPT, Moco is formed (Mendel 2013). The chemical structure of Moco can be found in the Figure 3 (adopted from NIH 2019).

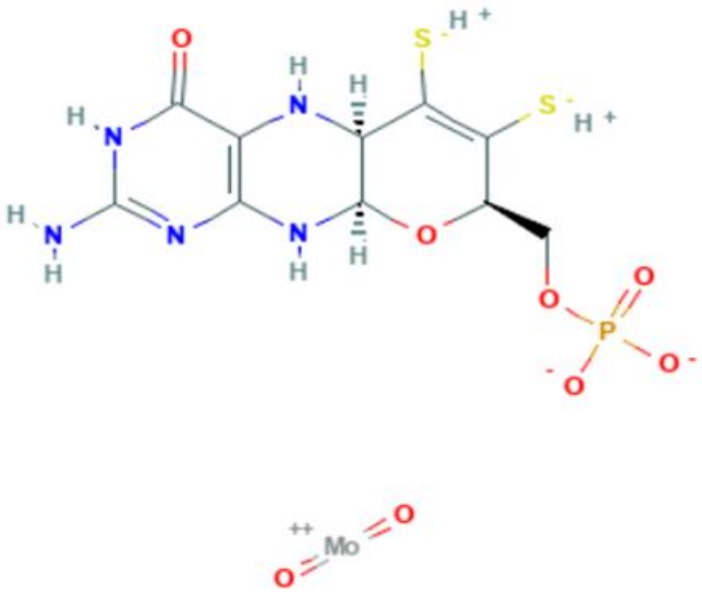

Figure 3. Chemical Structure Depiction of Moco

2.3.3 Molybdenum Uptake in Cells

Molybdenum is taken up in the forms of its oxyanion molybdate (MoO_4^{-2}) (Mendel and Kruse 2012). Molybdate-transporting proteins have been identified in algae and plants. MoT1 is the first molybdate transporter identified in plant-type eukaryotic organisms, but it is absent in animal genomes. Recently another molybdate, MoT2, has been identified in the alga, Chlamydomonas reinhardtii that is also present in animals including humans. MoT2 (Mass: 65,354 Dalton) in humans support the functionality of both proteins as molybdate transporters (Tejada-Jimenez et. al., 2011). Two proteins (Mot 1 and Mot 2) belonging to the large sulfate carrier superfamily are shown to transport molybdate with ultra-high affinity (500 nanomolar k_M value)

across cellular membranes. Unexpectedly, none of them (Mot 1 and Mot 2) was found to reside in the plasma membrane surrounding the cell (Mendel and Kruse 2012).

2.3.4 Molybdenum Cofactor Biosynthesis

There are six gene products which are involved in the biosynthesis (the synthesis of organic compounds within a living organism) of Moco in bacteria, fungi, plants, and humans. Only four genes are required for biogenesis (a principle that living organisms are produced only from other living organism) of Moco in humans. Humans genes and gene products follow the molybdenum cofactor synthesis (MOCS) nomenclature (MO cofactor synthesis) while in plants and fungi other forms of nomenclature as shown in the Figure 4 have been used (Maert and Wedd 2014). The Moco synthesis in humans has a high degree of similarity to the Moco synthesis in bacterium, and other organisms.

The Moco in all higher organisms is synthesized by a conserved biosynthesis pathway that can be divided into four steps. They are: cPMP; also known previously as precursor Z), MPT, adenylated MPT (MPT-AMP), and Moco as show in the Figure 10 (adopted from Mendel 2013). Four steps are described below very briefly.

Step 1: Conversion of GTP to cPMP

In human conversion of GTP to cPMP is catalyzed by protein MOCS1A.

Step 2: Synthesis of Molybdoprotein

In the second step, sulfur is transferred to cPMP to generate MPT.

Step 3: Molybdenum Insertion starts with Adenylation of Molybdoprotein

After MPT is synthesized, the chemical backbone is built and coordinate the molybdenum atom. Consequently, in the third step molybdate is transferred to MPT to form Moco. In this case, MPT-AMP is produced.

Step 4: Molybdenum insertion into Molybdoprotein

The final step involves MPT-AMP being transferred from G-do-main of Cnx1 to the E-domain, which cleaves the adenylate from MPT and catalyzes the insertion of molybdate into the dithiolene group of MPT, thus resulting in active Moco.

The Moco biosynthesis is described in detail elsewhere in the literature (Mendel and Kruse 2012).

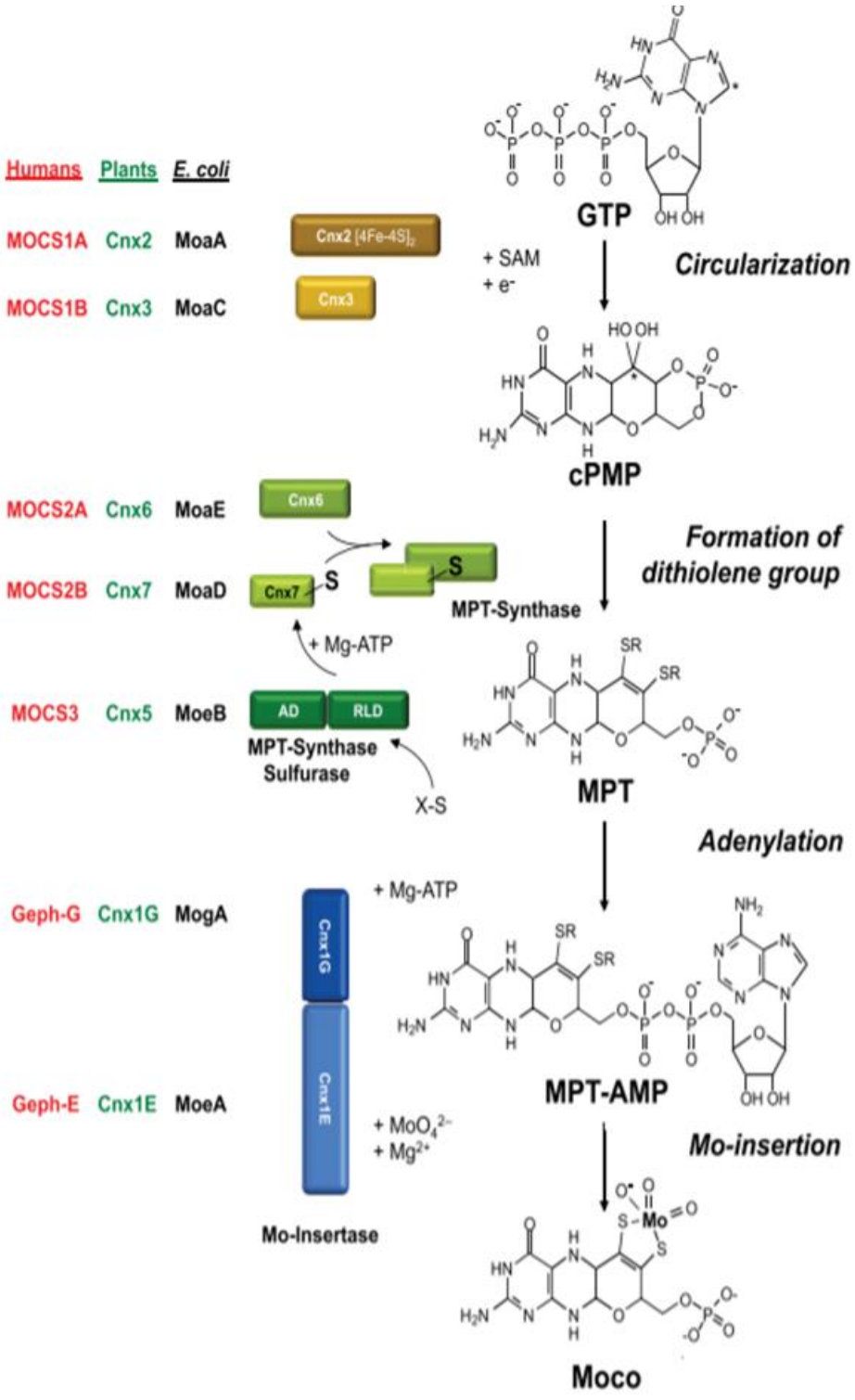

Figure 4. Biosynthesis of Eukaryotic Moco (Adopted from Mendel 2013)

2.3.5 Storage and Transfer of Moco

Proteins are often used in metal storage since they can bind and release metals under specific conditions via protein-protein interactions, pH changes, or cellular actions. Furthermore, proteins provide a suitable environment to control metal solubility and reactivity (Maert and Wedd 2014). The fast flow of Moco to its target enzymes is an essential prerequisite to reduce the threat of Moco degradation (Mendel 2013). The eukaryotes, Moco carrier Protein (MCP) was identified in the alga C. reinhardtti. The Moco carrier protein binds and protects Moco against oxidation. MCP forms a homotetramers capable of holding four molecules of Moco. As such, without any denaturing procedure, the subsequent transfer of Mocco from the carrier protein to aponitrate reduction (a complex molybdenum cofactor) from neurospora crassa (a red bread mold of phylum Ascomycota) is possible (Mendel 2013).

2.4 Modeling Methodology

Currently, dosimetrists use biokinetic models to describe the distribution, clearance, and organ retention of internalized radionuclides.

2.4.1 Biokinetic Methodology in Internal Dosimetry

Biokinetic models provide a mathematical means of predicting the distribution, retention, and clearance of contaminants within the body. Assessment of internal hazard can be understood by knowing two key pieces of information: the number of transformations occurring in an organ, and energy deposited per transformation. As such, it also requires interpretation of monitoring data in terms of intake and/or internal dose by considering many influencing factors, such as the physical and chemical speciation, route of intake, biokinetic, and energy absorption processes (Doerfel el al., 2002).

The International Commission on Radiological Protection (ICRP) and National Council on Radiation Protection and Measurements (NCRP) have developed and recommended various biokinetic models to assist in assessment of intake and doses from bioassay and monitoring data. Such biokinetic models are either generic or pre-systemic models which represent the behavior of various radionuclides after entering the human body via an intake pathway, or systemic models which describe the translocation of radioactive material after the direct uptake into the blood. The biokinetic models are revised as necessary when new data and information are available (Poudel 2016).

2.4.2 Biokinetic Model for Molybdenum

The whole-body retention R(t) of molybdenum in humans was described by ICRP publication 30 (Equation 3). This notation function was based on human data. Considering molybdenum translocated to organs or tissues, fractions of 0.1 and 0.9 were assumed to be retained with half-lives of 1 and 50 days, respectively. A biokinetic model of molybdenum was published in ICRP 134, part 2 (Figure 5).

$$R(t) = 0.1\, e^{-0.693t/1} + 0.9\, e^{-0.693t/50} \qquad \text{Eq (3)}$$

Where, R(t) = whole-body retention fraction

t = Retention time in days

The structure of the model consists of several compartments to describe the available data for molybdenum in-blood plasma, liver, kidneys, urinary bladder, and a generic tissue pool. Skeleton is not a major repository for molybdenum. As a consequence, skeleton was pooled together with the rest of the systemic tissues, excluding the liver, in a generic common compartment (Figure 5). Likewise, transfer coefficient parameter values in the systematic model for molybdenum are provided in ICRP 134 part 2 (Table 2). A urinary: fecal excretion ratio of 8:1

was assumed for molybdenum that has entered the blood compartment. No allowance for age-sex-dependence was provided in this model (ICRP 2016).

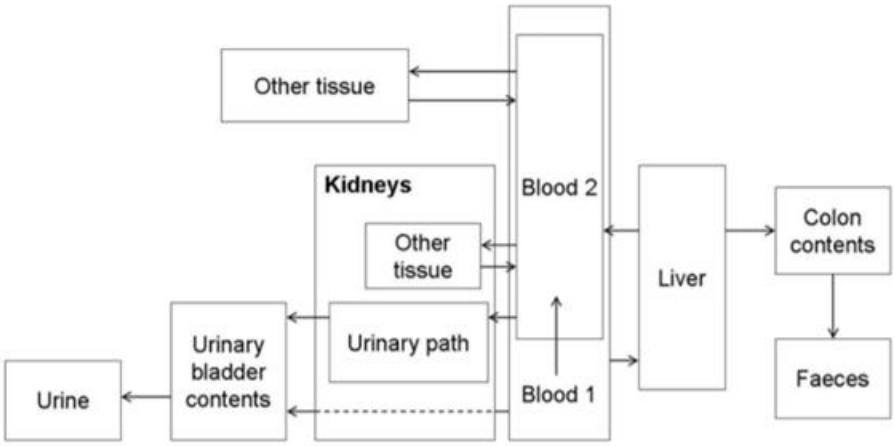

Figure 5. Systemic Model for Molybdenum Radionuclide (Adopted from ICRP 134, part 2)

Table 2. Parameters Values in the Systematic Model for Mo (ICRP 134, Part 2)

From	To	Transfer coefficient (per day)
Blood 1	Blood 2	12.5
Blood 1	Liver	14.2
Blood 1	Urinary bladder contents	6.5
Blood 2	Urinary path	1.7
Blood 2	Other kidney tissue	0.115
Blood 2	Other tissue*	1.73
Liver	Right colon tissue	0.0048
Liver	Blood 2	0.0122
Other Kidney tissue	Blood 2	0.0474
Other tissue	Blood 2	0.0323
Urinary path	Urinary bladder contents	1.4

2.4.3 Revised Biokinetic Model of Molybdenum by Giussani et al., 2004

A revised biokinetic model for molybdenum was published by Giussani et al., 2004 (Figure 6) using the series of investigations conducted directly in humans using stable Mo isotopes as tracers. This revised model consists of 6 compartments: 2 compartments are used to describe the transfer compartment (TC), taken to represent blood plasma and body fluids. Compartment 3 comprises the organs and tissues which exchange materials with TC. Compartments 4 and 5

represent kidney, and passage from 4 to 5 describes the process of storage in that organ. This process is considered to be best described by saturable nonlinear kinetics, which explains why, at higher amounts of circulating molybdenum, the fraction which is directly excreted from compartment 4 to compartment 6 increases.

Giussani et al., 2004 formulated equation 4 to describe the saturable kinetics of molybdenum. Transfer coefficient values used in the revised biokinetic model can be found in Table 3. The f-1 value (fraction absorption from the gastrointestinal tract) used was 0.88.

$$K_{54} = k_a * \left[1 - \frac{q_5}{k_b}\right]^{3 \cdot 5} \qquad \text{Eq (4)}$$

Where, q_5 is the amount of total molybdenum in compartment 5, k_b is the saturation amount which is equal to 90 µg, and k_a is a constant (Giussani et al., 2004). Likewise, transfer coefficient parameter values derived by Giussani et al., 2004 are given in Table 4.

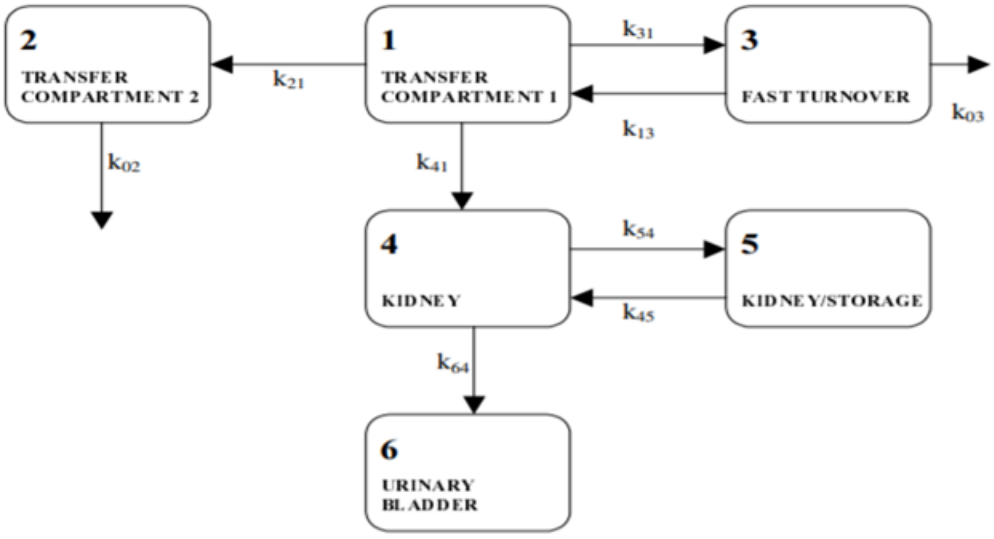

Figure 6. Revised Biokinetic Model of Molybdenum (Giussani et al., 2004)

Table 3. Numerical Values used in Revised Mo Biokinetic Model (Giussani et al., 2004)

Parameter	Value per min	Parameter	Value per min
k_{21}	0.0023	k_{03}	0.0023
k_{02}	8.12×10^{-4}	k_{41}	0.0096
k_{31}	0.0094	k_{45}	8.19×10^{-5}
k_{13}	0.036	k_{64}	0.011
k_a	0.018		

The revised model suggests that urinary excretion is very fast and occurs mostly within first the few hours and at 48-hours excretion is negligible. Furthermore, molybdenum excretion increases with the increasing amount of circulating molybdenum. This finding is contrary to the ICRP model which suggests slower elimination via the renal pathway, with less than 7% eliminated over 48 hours, and 14% over one-week (Giussani et al., 2004). The revised model also suggests that excretion of systematic molybdenum (molybdenum already stored in the body) is also enhanced, if the administered amount of molybdenum is increased.

2.4.4 PBPK Modeling Methodology

A physiologically based pharmacokinetic (PBPK) modelling is another approach to describing the biological behavior of a substance. Figure 7 is a simple diagrammatic scheme of the PBPK model.

2.4.4.1 PBPK Modeling

PBPK modeling is used in the pharmaceutical industry for the development of drugs by predicting their absorption, distribution, metabolism, and elimination (ADME) (Kuepfer et al., 2016). Likewise, PBPK models are the mathematical descriptions of how a chemical enters the body, the amount of chemical that gets into the blood, how the chemical moves between body tissues and the blood, and how the body metabolizes and eliminates the chemical (EPA 2018). The

PBPK models incorporate information about the body's anatomical and physiological structures as well as biochemical processes into the model structure (EPA 2018).

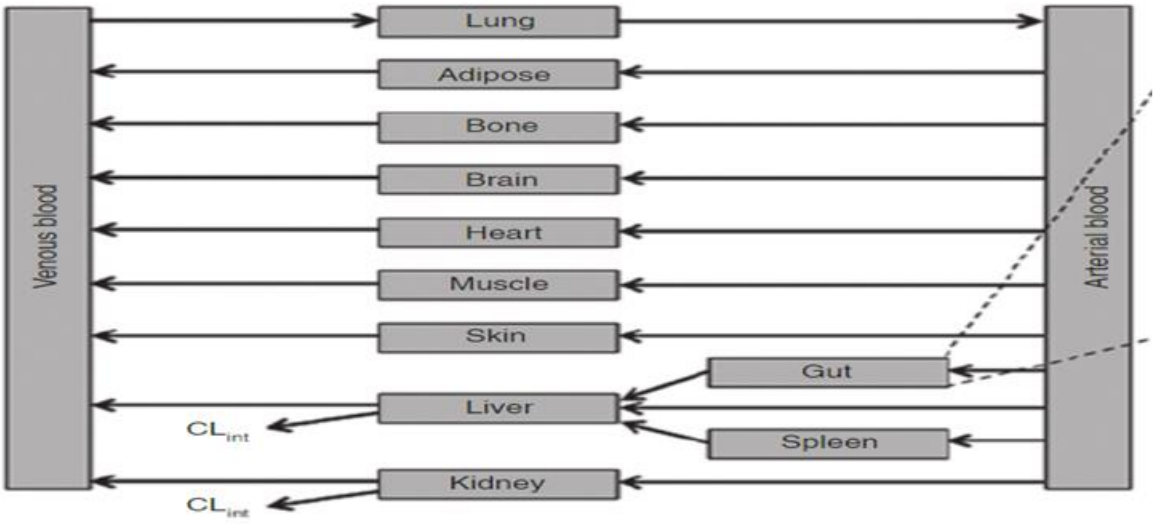

Figure 7. PBPK Model of a Human System (Adopted from Kuepfer et. al., 2016)

A PBPK model consists of compartments representing tissues in the body, connected by the circulating blood system as shown in the Figure 7. The dotted lines represent subdivision of gastrointestinal tract (GUT) as shown in Figure 10. Each compartment is defined by a tissue volume, and tissue blood flow rate (Jones and Rowland-Yeo 2013). A PBPK model includes the main tissues of body, adipose, bone, brain, gut, heart, kidney, liver, lung, muscle, skin, and spleen. In some cases, reduced models (Figure 8) have been used in some cases that lump tissues with similar tissue absorption characteristics together to reduce the number of compartments and overall complexity of the model (Cao et al., 2013). Compound specific characteristics implemented in traditional PBPK modelling include lipophilicity, molecular weight, and solubility (Figure 9). Physiological parameters include blood flow rates, organ volumes, and tissue surface areas (Kuepfer et al. 2016). The mode of administration (i.e., route of entry) is also taken into consideration in PBPK modelling. Some components such as formulation, administration protocol, and special events (such as food, and exercise) as shown in Figure 9 are optional

depending on the model considered. In PBPK modeling, mass conservation principles among the compartments are used.

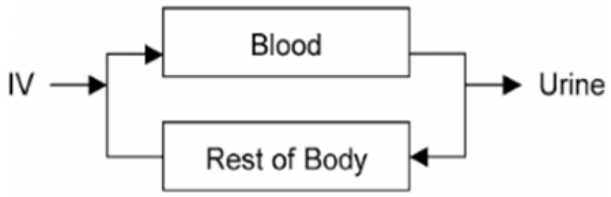

Figure 8. An Example of a Two Compartment PBPK Model (Adopted from Clark et. al., 2004)

Depending on the anatomical structures and functional role, an organ can be subdivided into multiple parts. Figure 10 shows that the gastrointestinal tract is subdivided into several segments: stomach, small intestine, upper and lower jejunum, etc. Each of these segments can be further divided into zones as shown in the Figure 7. Similar division and subdivision approaches can be applied to any organs such as the kidney, liver, etc. as required.

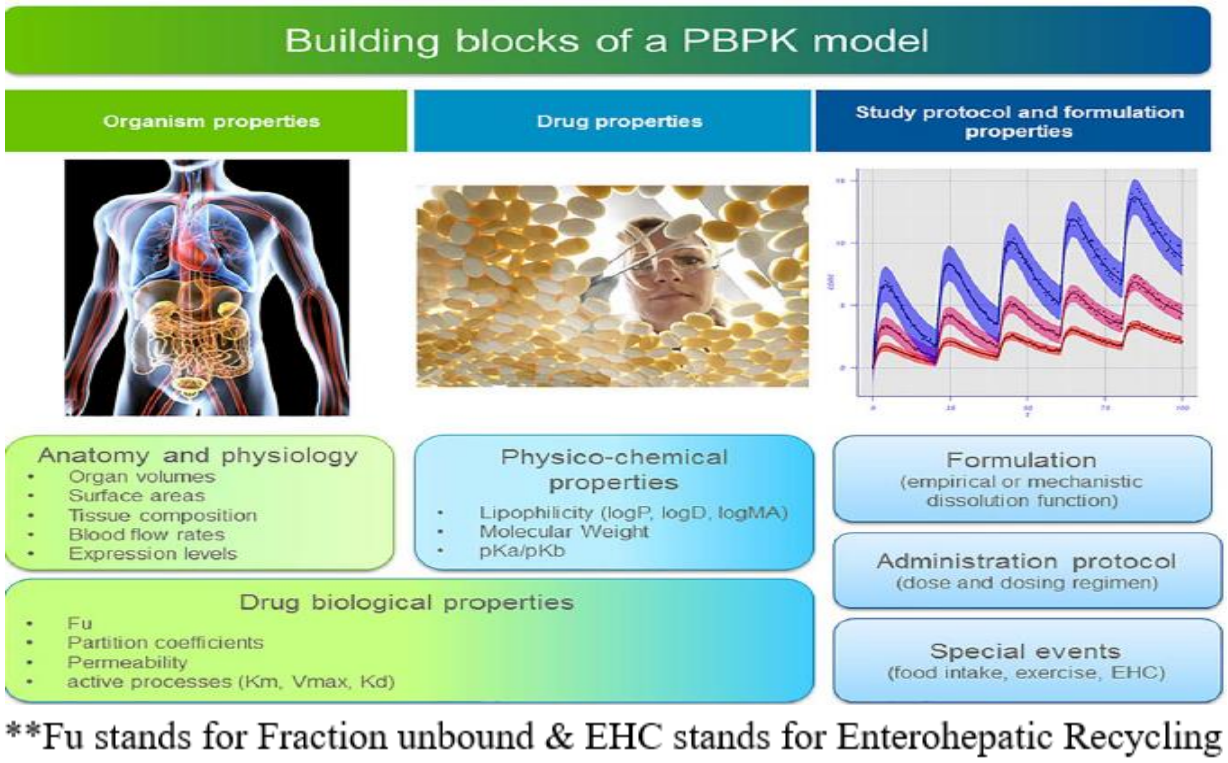

Figure 9. Important Components of PBPL Model (Adopted from Kuepfer et. al., 2016)

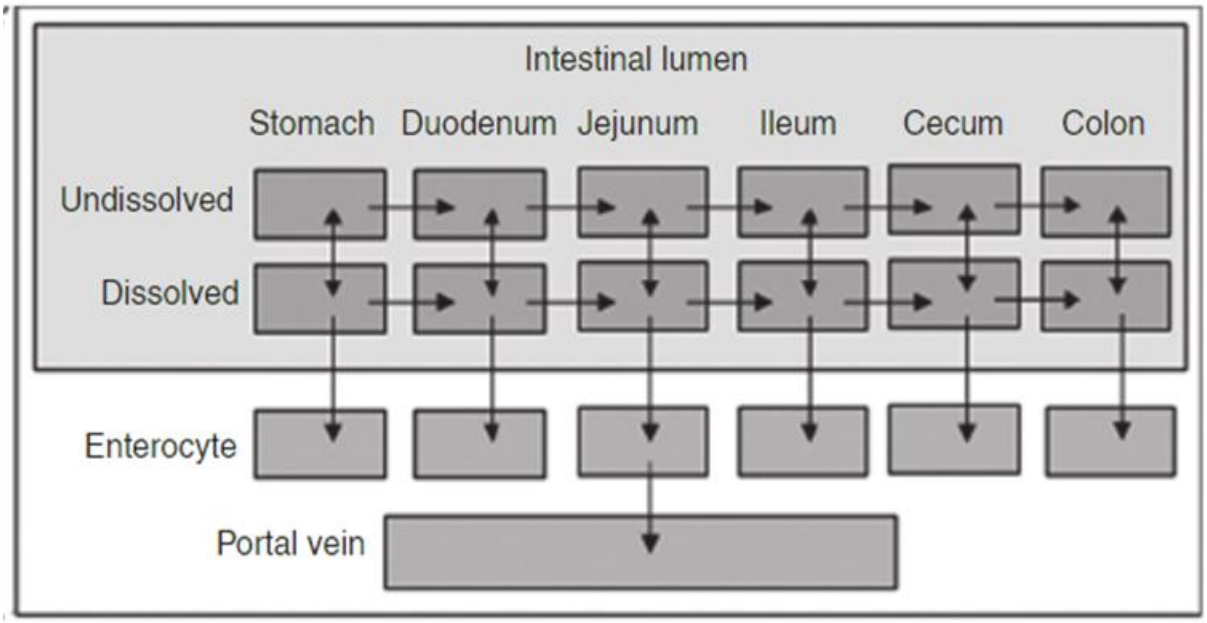

Figure 10. Subdivision of Gut for PBPK modelling (adopted from Kuepfer et al., 2016)

There are two fundamental parameters for building a PBPK model: clearance and volume of distribution. Clearance (CL) is defined as the volume of plasma from which the drug has cleared over a period of time (Jones and Rowland-Yeo 2013). Total clearance as shown in equation 5 is the summation of clearance via fecal and urine excretion as well as the metabolism of the drug (Jones and Rowland-Yeo 2013). Whereas the volume of distribution refers to the volume of plasma required to occupy the total amount of drug in the body at the concentration observed in plasma. Volume of distribution and clearance can be used to determine the effective half-life or residence time of the drug (Jones and Rowland-Yeo 2013).

$$CL_{total} = CL_{hepatic} + CL_{renal} + CL_{other} \quad \text{(Eq 5)}$$

Although there are differences in models, biokinetic and PBPK models are comparable as they both model biological behaviors. The delivery rate from arterial blood to kidneys tissues for example in a PBPK model is comparable to the transfer rate between the blood and kidney tissues in ICRP compartmental models. As such, the return of activity from the kidney tissue compartment

to the central compartment described in ICRP is instead denoted as transfer to the venous blood in a PBPK model. These similarities enable the validation of transfer coefficients to support of ICRP models.

2.5 Compartmental Models

The human body can be categorized into compartments with individualized volume, xenobiotic concentration in the compartment, and by chemical reactions. Rate constants of mass transfer can be used to characterize translocation among the compartments. The system can also include input and output functions representing administration/exposure and clearance. The major function of the simplified compartmental model is to describe the time function of the plasma concentration in a mathematical expression. The concentration at any time after intake is a function of the initial dosage and the physiological processes of ADME (Riviere 1997).

2.5.1 One Compartmental Model

The simplest model is a one compartmental model where the drugs is evenly distributed to tissues and fluids within the body (Figure 11, adopted from Riviere 1997). The entire body acts like one uniform compartment in a one compartmental model. Likewise, in a one compartment model, a drug can enter, and leave the body via excretion. The fate of a drug or other substance that distributes instantaneously and evenly in the body in this type of model that is eliminated at a rate and amount that is proportional to the amount left in the body can be determined (Figure 12, adopted from NIH 2020). This phenomenon is a first order rate expression and can be represented as the logarithm of concentration in blood as a liner function of time as shown in Figure 12. The equation for a straight-line clearance in Figure 12 can be computed using Equation 6. Furthermore, half-life ($T_{½}$) of the chemical drug can be calculated using equation 7. Also, from the biological perspective, the half-life also can be calculated using the Equation 10 (Riviere 1997).

$$\text{Concentration}(C) = Ae^{-kt} \qquad \text{Eq (6)}$$

$$T_{1/2} = \frac{0.693}{k} \qquad \text{Eq (7)}$$

Where, A is the concentration intercept (mass/volume) at time zero, K is the slope (unit 1/time), and t is the time after injection.

As such, volume of distribution (unit of volume) and clearance (unit of volume/time) can be computed using Equation 8 and 9, respectively.

$$Vd = \frac{Dose}{A} \qquad \text{Eq (8)}$$

$$CL = K^* Vd \qquad \text{Eq (9)}$$

Where, Vd and CL are volume of distribution and clearance, respectively.

$$T_{1/2} = \frac{0.693 * Vd}{CL} \qquad \text{Eq (10)}$$

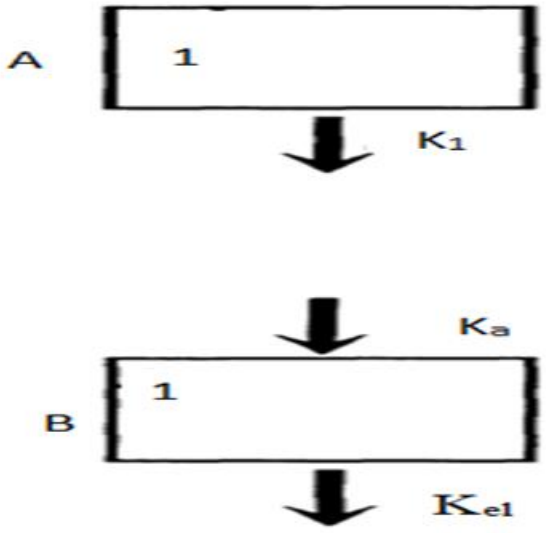

Figure 11. Diagrammatic scheme of one compartmental model (A: Intravenous dosing, B: Extravascular dosing, K_a: rate Constant, and K_{el}: elimination rate)

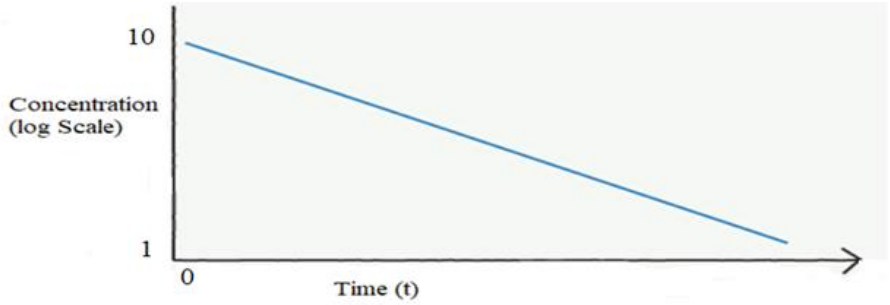

Figure 12. One Compartment Model

2.5.2 Two Compartmental Model

Most of the drugs are not described by a one compartment model because the plasma concentration-time profile is not linear. The human body is not a single homogenous compartment. Instead, it is composed of regions that are defined by having different rates of drug distribution (Riviere 1997). This complicated situation can be solved using a two compartmental model.

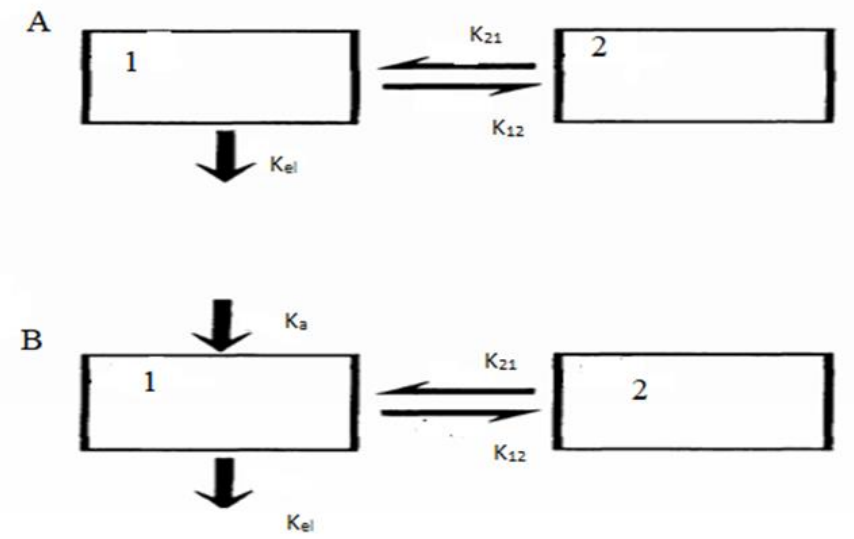

Figure 13. Diagrammatic scheme of a two compartmental model A: Intravenous dosing, B: Extravascular dosing, K_{12} &K_{21}: rate out of compartment 1 and in to 2 & rate out of compartment 2 and in to 1, K_a: rate Constant, and K_{el}: elimination rate)

Two compartmental models, based on basic principle of mass balance, are used mostly to describe the kinetics of chemicals and other substances (Figure 13, adopted from Riviere 1997). Two compartmental models are used for drugs which distributes slowly within the body (NIH 2020). The drug or other substance enters and distributes in the first compartment. It is then distributed to another compartment. The concentration in the first compartment decreases with time. However, the concentration in the second compartment rises, peaks, and also decreases as the drug is eliminated from the body as shown in Figure 14 (NIH 2020).

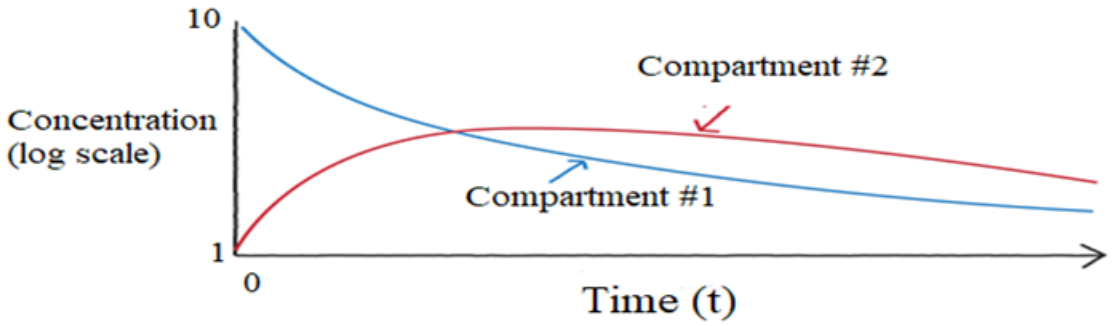

Figure 14. Two Compartment Model

The strategy in a two compartmental model is to infuse a drug into the body at a constant rate R_0 (mass/time) and then measure the plasma drug concentrations. When a steady state plasma level is achieved, the rate of drug input must be equal to the rate of clearance from the body as shown in Equation 11.

$$R_o = C^{ss} * CL \qquad \text{Eq (11)}$$

Where, C^{ss} is the steady state plasma level (mass/time)

Rearranging Equation 11 gives the equation to calculate CL in Equation 12.

$$CL = R_o / C^{ss} \qquad \text{Eq (12)}$$

2.5.3 Three Compartmental Model

Depending on the need, a model can be divided into three compartments as shown in the Figure 15 (adopted from Riviere 1997). The drug in figure 15 distributes into two different compartments. A third compartment is usually a so-called deep compartment characterized by a slow rate constant. The drug is always eliminated from the central compartment and a dose of the drug is always administered into the central compartment. The three-compartment model has six rate constants as shown in the Figure 15. These models can get even more complicated if simultaneous urine and tissue sampling occurs.

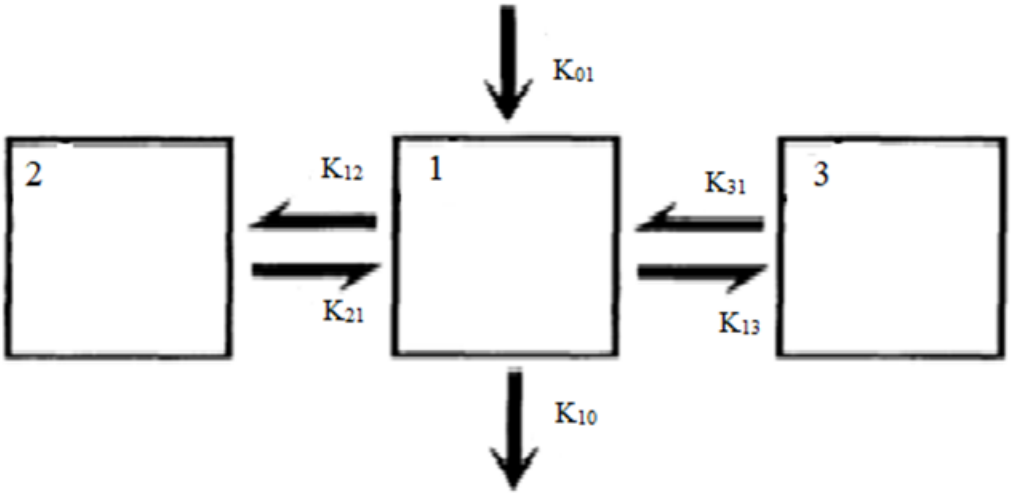

Figure 15. Diagrammatic Scheme of Three Compartmental Model

where, (K_{12}, K_{21}, k_{31}, k_{13} are transfer rate constants from compartment to another, K_{01}: rate Constant, and K_{10}: elimination rate)

2.6 Kidney and Urine Formation

Kidneys are a pair of bean-shaped organs, each about the size of the fist. They are located just below the rib cage, one on each side of the spine. Healthy kidneys filter about half a cup of blood every minute, removing wastes and extra water to make urine. The urine flows from the

kidneys to the bladder through two thin tubes of muscle called ureters, one entering on each side of the bladder (NIH 2020).

2.6.1 Formation of Urine

The formation of urine involves three major processes. They are glomerular filtration, tubular reabsorption, and tubular secretion.

2.6.1.1 Glomerular Filtration

Filtration is a process in which blood pressure forces plasma, and dissolved substances, and small proteins out of the capillaries. Blood pressure in the glomerular filtration forces plasma, dissolved substances, and small proteins out of the glomeruli and into Bowman's capsules. This fluid is no longer plasma, but it is called renal filtrate. The blood cells and larger proteins are too large to be forced out of the glomeruli, that being the case, they remain in the blood. Useful materials such as nutrients and minerals are also dissolved in plasma and are present in renal filtrate. Filtration is not selective with respect to usefulness; it is selective only with respect to size. Therefore, renal filtrate is much like blood plasma, except that there is far less protein, and no blood cells are present (Scanlon and Sanders 2007).

Glomerular filtration rate (GFR) is the amount of renal filtrate formed by the kidneys in one minute, and this averages 100 to 125 mL per minute. GFR can be altered if blood flow through the kidney changes (Scanlon and Sanders 2007).

2.6.1.2 Tabular Reabsorption

Tubular reabsorption is the process by which the nephrons remove water and solutes from the tubular fluid (pre-urine) and returns them to the circulating blood. Approximately 99% of the filtrate is reabsorbed back into the blood in the peritubular capillaries. Only about 1% of the filtrate will enter the renal pelvis as urine (Scanlon and Sanders 2007).

The ureters, urinary bladder, and urethra do not change the composition or amount of a urine but play a role in the collection and periodic elimination of urine.

2.7 Model Comparisons using Statistics

2.7.1 Akaike Information Criterion (AIC)

AIC is a way of selecting a model from a set of models. The AIC compares the quality of a set of statistical models to each other. The AIC will take each model and rank them from best to worst (Statisticshowto 2020). Moreover, based on AIC criteria, best model will be neither under-fit nor over-fit. The absolute quality of the model cannot be obtained using the AIC model. As such, if all the models are bad, it will select the best out of a bad bunch. A lower AIC score is better while comparing one fit to another. AIC is low for models with high-likelihood values, but adds a penalty term for models with higher parameter complexity, since more parameters means a model is more likely to overfit to the given data. The AIC is calculated using Equation 13 (Medium 2020).

$$AIC = -2(\text{log-likelihood}) + 2K \qquad \text{Eq (13)}$$

Where, K is the number of model parameters (the number of variables in the models plus the intercept), and Log-likelihood is a measure of model fit. The higher the number of log-likelihood parameter, better is the fit.

The second order information criterion, often called AIC_c, considers sample size by increasing the relative penalty for model complexity with small data sets (about less than 40). AIC_c can be calculated using Equation 14.

$$AICc = -2(log - likelihood) + 2K\left(\frac{n}{n-K-1}\right) \qquad \text{Eq (14)}$$

Which can be simplified as (Equation 15):

$$AICc = AIC + \frac{2K(K+1)}{N-K-1} \qquad \text{Eq (15)}$$

Where, n is the sample size, K is the number of model parameters, and Log-likelihood parameter is the measure of model fit. As n gets larger, AIC_c converges to AIC, and consequently there is no harm in always using AIC regardless of sample size.

2.7.2 Delta AIC Scores

AIC scores are reported ΔAIC or Akaike weights. The ΔAIC is the relative difference between the best model which has a (ΔAIC of zero) and each other model as shown in equation 16 (Statisticshowto 2020).

$$\Delta AIC = AIC_i - \min AIC \qquad \text{Eq (16)}$$

Where, AIC_i is the score for the particular model I, and min AIC is the score for the best model, respectively. The best model will therefore have a $\Delta AIC \geq 0$. A low ΔAIC value for model i indicates that the model has a comparable predictive power to the best model. As such, high ΔAIC indicates that there is little evidence to support model i (Burnham and Anderson 2002).

2.7.3 Akaike Weights

Akaike weights can be used in model averaging. They represent relative likelihood of a model. The relative likelihood can be calculated by using Equation 17.

$$e^{-\frac{1}{2}(AIC_i - AIC_{min})} \text{ or } e^{-\frac{1}{2}(\Delta AIC)} \qquad \text{Eq (17)}$$

AIC_i can be greater than or equal to AIC_{min}. The relative likelihood of a model can be defined by a normalized set of positive quantitative parameters called Akaike weights as shown in Equation 18. The Akaike weight of a particular model "i" can be calculated by dividing its relative likelihood by the sum of all the relative likelihood values in the model set R, where the calculated w_i for all models of interest must add up to 1 (Burnham and Anderson 2002).

$$W_i = \frac{e^{-\frac{1}{2}(\Delta AIC i)}}{\sum_{r=1}^{R} e^{-\frac{1}{2}(\Delta AIC)}} \qquad \text{Eq (18)}$$

An Akaike weight of 1 means that a particular model is about 100% more accurate and it more likely to be the best approximating model for a given data set compared to other models of interest. An Akaike weight of 0.5 means that there is about a 50% chance for a particular model to be the best representation of the dataset when compared to the model of interest. Consequently, the model with the largest Akaike weight is considered the best model among the model set (Burnham and Anderson 2002).

CHAPTER 3. METHODS AND MATERIALS

3.1 Data Used: Monitoring of Accidental molybdenum Exposure

^{99}Mo and ^{99m}Tc were accidently inhaled by a group of seven workers belonging to a company manufacturing of ^{99m}Tc generators for use in nuclear medicine in. The retention and excretion data used in this project was published in 2004. During the accident, workers were handling a ^{99}Mo source, and they inhaled a radioactive aerosol containing ^{99m}Tc and ^{99}Mo. Monitoring procedures included whole body counting and collection of urinary and fecal samples. Pure ^{99}Mo (half-life of 66 hours) immediately decays to ^{99m}TC (half-life of 6.6 hours), and in several hours transient equilibrium were reached. The first measurements were performed 1.3 days after the accident happened. The 140 keV from ^{99m}Tc with an assumption of transient equilibrium with ^{99}Mo were counted. Estimations of intake and doses were made using a model based on ICRP 30 publication. ^{99m}Tc contributed due to the transient equilibrium with its parent but made no significant difference in the total dose. Whole body (WB) measurements were performed at the shielded room of the Whole-Body counting facility of the Center for Energy, Environment and Technology (CIEMAT) in Spain, using a NaI(Tl) detector system. Counting times of 1200 seconds were used with the individual in a reclined-chair geometry. Urine data was expressed as daily excretion. Data extrapolations were made using the measurements from spot samples (Alvarez et al., 1994 and Giussani et al., 2004). These are the only available human data regarding molybdenum and technetium exposure found during this research.

Data used in this project were interpreted from Figure 16 (see Appendix 1.1 for data points), and Figure 17 (see Appendix 1.2 for data points) which were published in Giussani et al., 2004. The different shapes and colors in Figure 16 and 17 represent different individuals whose urine was collected. These individuals also received whole-body counting. The percentage of

whole-body retention of inhaled molybdenum was estimated using the systematic model of ICRP. This is plotted against time after incorporation in days in Figure 16. Figure 17 provides the cumulative 24-hour urine excretion of inhaled molybdenum calculated with the systematic model of ICRP is plotted against time after incorporation. Data were extrapolated from the measurement of spot samples, assuming a daily excretion volume of 1.4 L.

For the analysis of the data collected in the exposed workers, the cumulated 24-hour urinary excretion was simulated using the urinary bladder data, forcing the bladder emptying at the time when sample collection was started, and integrating for 24 hours. Similarly, the integration of spot samples was performed over 3-hours, and the result multiplied by 8 in order to get the daily excretion, since no information on the sampling duration nor on the volume excreted had been kept at the time of accident. The whole-body retention data was calculated at the time when the WB measurements was started considered (Giussani et al., 2004).

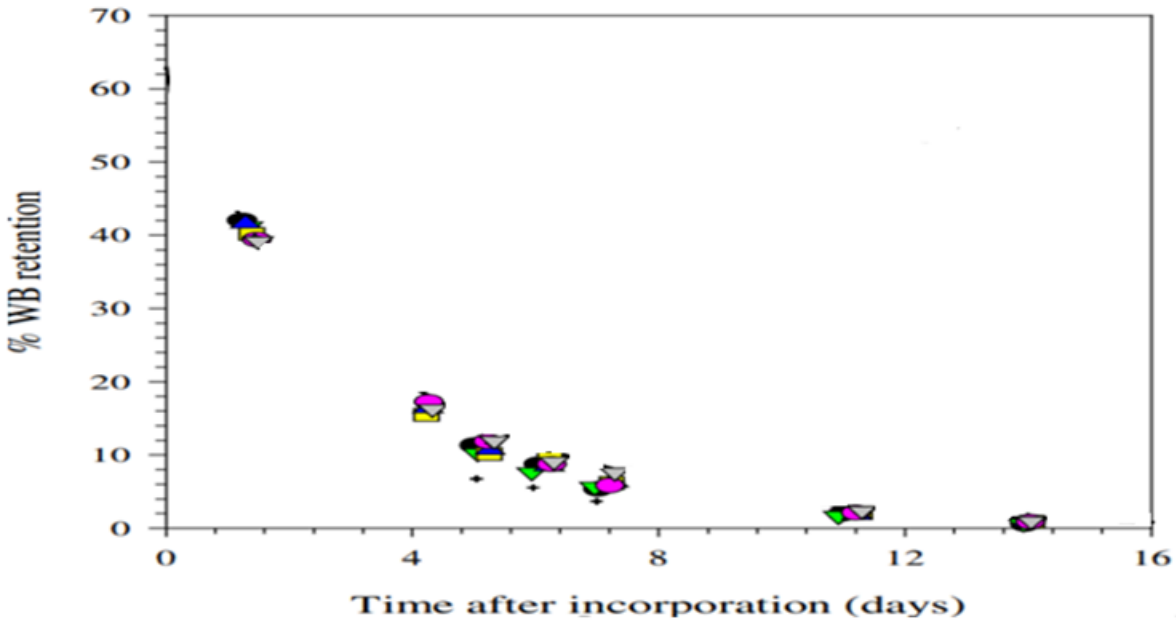

Figure 16. Whole Body Retention Data Used in this Project (From ^{99}Mo, and ^{99m}Tc at equilibrium)

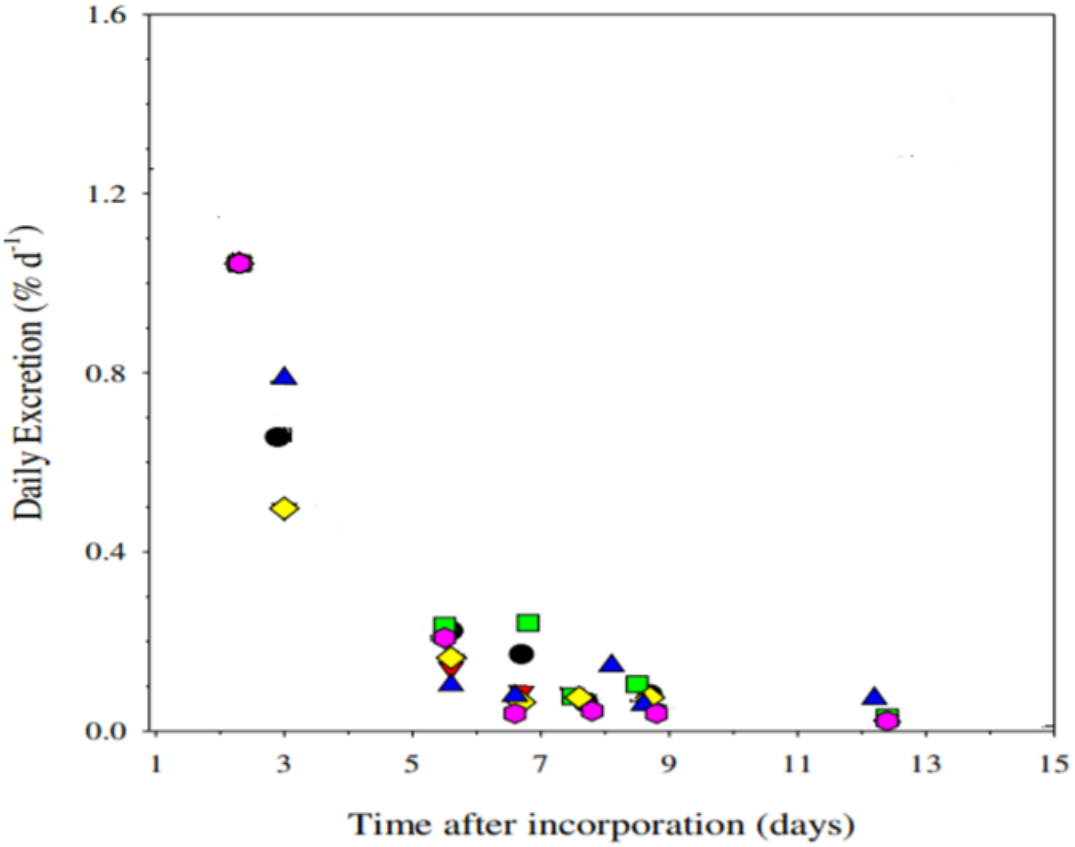

Figure 17. Daily Excretion data used in this project (from ^{99}Mo, and ^{99m}Tc at equilibrium)

3.2 Model Identification/Structure used in this Research

A PBPK based molybdenum models can be proposed in many ways. However, eight and six compartmental PBPK based models (model-A and model-B) were proposed, by considering the functions of the kidneys (described in section 2.6) in the human being, as shown in Figure 18 and 19, respectively. To test the performance of the proposed PBPK models, model-A, and model-B were constructed in SAAM II (described in section 3.5) and compared with each other using AIC values[6]. The ICRP model (Figure 5) and the Giussani model (Figure 6) were reconstructed in

[6] Licensed to University of Washington, SAAM II, Simulation, Analysis, and Modeling Software, Version-2, Serial Number: PC1509, Accessed July 2020-May-2021

SAAM II by using the transfer coefficient values listed in Table 2, and 3, respectively. The AIC values obtained from the SAAM II were used to evaluate which model (out of four) provided the largest AIC parameters values.

The tissues and organs with similar tissue absorption characteristics were pulled together in one compartment. Depending on the anatomical structures and biological functions, some organs or tissues were ignored or excluded from modeling. To develop a PBPK model, the following assumptions have been made. Assumptions 2, 3, and 4 supports the idea that the glomerular filtration is dominant in molybdenum filtration.

Assumption 1: 80% of inhaled molybdenum is absorbed in a plasma (ICRP 30, part I)[7]

Assumption 2: All molybdenum is specifically bound to an alpha-2 macroglobulin instantaneously (Kselikova et al, 1980).

Assumption 3: Kidney glomerular actively filter molybdenum with an alpha-2 macroglobulin.

Assumption 4: All other tissues do not accumulate molybdenum with alpha-2 macroglobulin.

Assumption 5: Molybdenum does not accumulate in the kidney.

Assumption 6: All of the molybdenum is eventually excreted in urine.

3.3 Proposed Model Structure

SAMM II was used to construct proposed model-A and model-B using a generalized PBPK structure as the basis for these molybdenum models. Both models primarily focused on renal systems. The primary distribution compartment is the blood plasma in both models (Figure 18 and 19). Molybdenum excretion occurring via the liver is negligible in both models. Since the liver has no significant role in these models, it is lumped with rest of the body (ROB). Skeleton too is of no importance in these models, and therefore it is lumped with ROB. In Figures 18 and 19, s1

[7] Source: ICRP 30 Part I Volume 2 No.3/4 page-83 1979

and s2 represent whole body and excretion sampling, respectively. The transfer rates between two compartments are labelled in SAAM II as “k(source compartment, target compartment)”. Likewise, ex1 represents the amount of activity inhaled.

About 80% of the molybdenum-99 aerosols inhaled and deposited in the lung is absorbed in plasma in a short period of time in both models, and rest of the molybdenum is exhaled. Molybdenum in the form of molybdate in plasma transfers to the rest of the body including the liver and skeleton and experiences recycling in both models. Molybdenum is also in the form of molybdate in plasma transfers to the kidney and to extra cellular fluid (K-ECF) and experiences recycling in both models. Molybdate from K-ECF directly goes to the bladder and experiences recycling in Model-B. Molybdate from K-ECF in Model-A goes to two different compartments, namely, the Granular compartment for granular filtration (GF) and Tubular compartment for tubular secretion and tubular reabsorption. If there is little or no significance of tubular secretion and tubular reabsorption, model-A simplifies to model-B. Model-B in other words is the equivalent of simplified organ model of model-A.

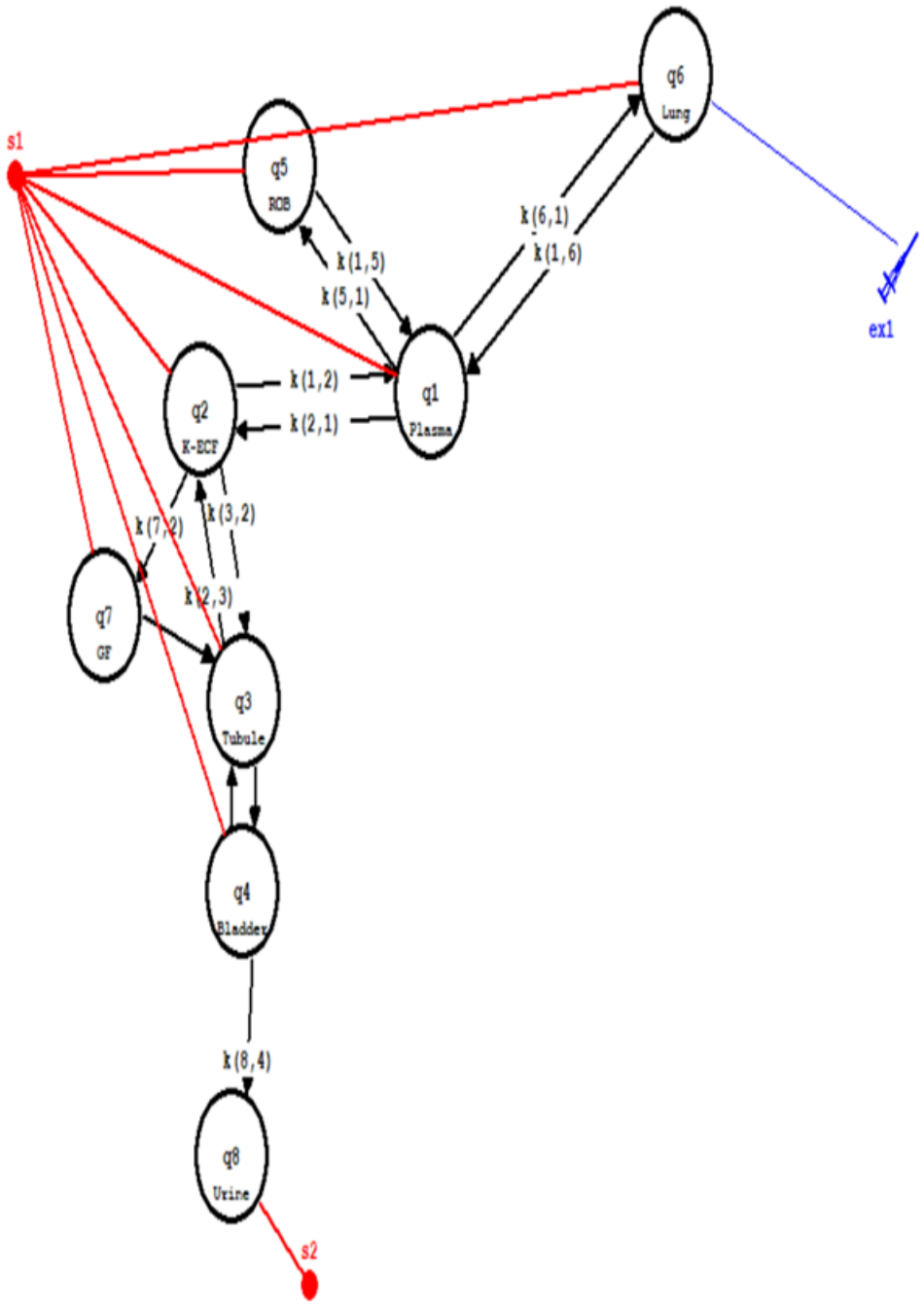

Figure 18. Proposed Model-A PBPK Model

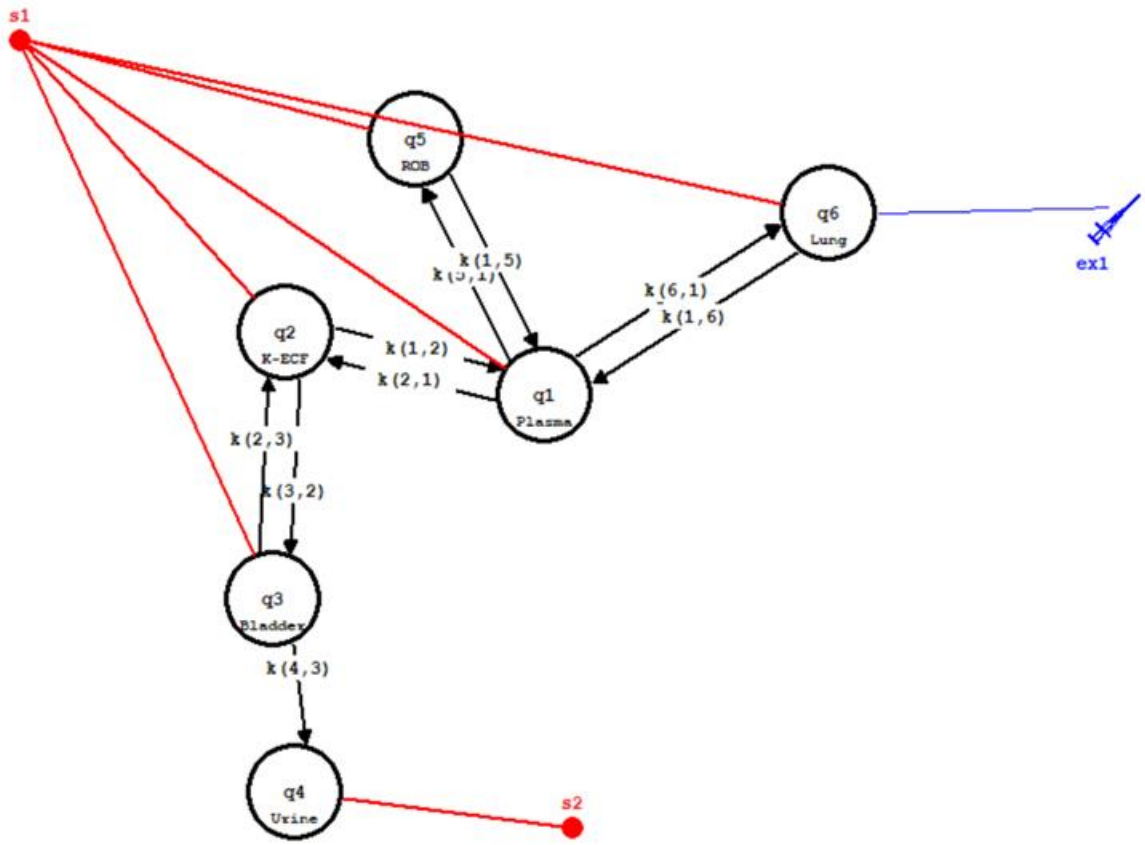

Figure 19. Proposed Model-B PBPK Model

3.4 Akaike Information Criterion (AIC)

The AIC statistic was used in this project to quantitatively evaluate the quality of the model. The AIC values were obtained from the SAAM II software and were used to evaluate the model fits. The lower values of AIC were desired while selecting the best model. In addition, concepts of ΔAIC and Akaike weights were also used to compare the models.

There were few other statistical techniques available such as Jackknife, and Chi-Square testing. The Jackknife is a method used to estimate the variance and bias of a large population, whereas the Chi-Square goodness of fit test determines if sample data matches a population. However, the technique of AIC was used. The secondary goal of this project was to compare proposed models with the Giussani model, and the ICRP model. AIC is the statistical technique

which can be used to compare from one model to another, hence was used in this project. AIC is equally good for small data set, which was the case in this project. The SAAM II software provides the values of AIC automatically, hence AIC was used for convenience, too.

3.5 Modeling Software

The SAAM II[8] software was used for this project. The SAAM II is a modeling, simulation, and analysis software package which supports the development and statistical calibration of compartmental models in biological, metabolic, and pharmaceutical systems. The SAAM II employs state-of-the-art numerical and statistical methods and algorithms. It is widely regarded as the most robust and accurate package for solving systems of differential equations and for fitting model parameters to experimental data sets with specified error models (TEG 2017). The SAAM II automatically gives the AIC values, which can be used to evaluate the quality of different models. There are several publications (see footnote 9) describing the studies which used the SAAM II software and can be used as a validation and verification of this software[9].

The SAMM II compartmental application allows a choice from set of model-building tools representing compartments, and transfer rates to build a graphical representation of a compartmental model on a drawing canvas. The SAAM II software automatically creates a system of differential equations from the model represented by this graphical representation. There are three integrators available in SAAM II to solve the model. They are: the Rosenbrock integrator (uses a semi-implicit default method), the Runge-Kutta (uses standard forward integrating order 5-4 method), and the Pade integrator (uses a method developed by the resource facility for Kinetic Analysis at the University of Washington and is based on the Pade approximation of the matrix

[8] Licensed to University of Washington, SAAM II, Simulation, Analysis, and Modeling Software, Version-2, Serial Number: PC1509, Accessed July 2020-May-2021
[9] https://tegvirginia.com/resources/publications/

exponential)[8]. The models developed during this analysis were solved using the Rosenbrock integrator that is a default recommended used in this code.

Rosenbrock integrator is a non-convex function which is used as a performance test problem for optimization algorithms. Rosenbrock integrators are an effective solution of initial value problems for stiff systems of ordinary differential equations (Shampine 1982).

CHAPTER 4. RESULTS AND DISCUSSIONS

4.1 Calculation of Transfer Rates

The transfer rates values (day^{-1}) for model A, and B were calculated by dividing the flow rates by the volume of the source compartment as shown in Table 4 and 5, respectively. The concept of mass balance was used to calculate the flow rates and the volume of the rest of the body (ROB). The transfer rates from the bladder to the kidney was assumed to be negligible in models A, and B.

4.2 Model Performance

Models (A, and B) were evaluated using the SAAM II software by using the data set obtained from Figure 16 and 17, and the transfer rate values obtained from Table 6 and 7. When employing model-A, three out of thirteen transfer rates required empirical fitting (Table 6). Various iterations for model-A in SAAM II were performed using the parameters in Table 6 until the best fit of the data was obtained. However, for model-B, no empirical fitting was required (Table 7). Three empirically obtained transfer rates, of model-A can be found in Table 8. The ICRP model (Figure 5) and the Giussani model (Figure 6) were reconstructed in SAAM II by using the transfer coefficient values listed in the Table 2, and 3, respectively. The values of AIC_{SAAM} were automatically obtained from the software for all the models. The formula SAAM II software used to calculate the AIC values was different than the one which was discussed in the literature review section (Equation 13). However, $AIC_{Literature}$ and AIC_{SAAM} values were interchangeable using the formula described in Appendix 2.1. The values of $AIC_{Literature}$ (described in Appendix 2.1), ΔAIC, Relative Likelihood, and Akaike Weight were calculated by using the equations in Appendix 2.1, Equation 16, Equation 17, and Equation 18, respectively (Table 9).

Table 4. Transfer Rates for Model-A

Blood distributions transfer rates in the humans (Model-A)					
Source Compartment	Target Compartment	Flow rate (L/Min)	Volume of source compartment (L)	Transfer rate (day^{-1}) [b]	Reference
[v]Plasma	Lung	6.08	4.42	1980	De Buck et.al., 2007
[a]Lung	Plasma	6.08	1.11	7890	De Buck et.al., 2007
[c]ROB	Plasma	4.83	76.1	91.4	Total Blood flow and total volume obtained from Buck et.al., 2007
[a]Plasma	ROB	6.08	2.21	3960	De Buck et.al., 2007
[da]Plasma	K-ECF	1.00	2.21	652	Douglas and Pooler 2016
Kidney-ECF	Plasma	1.02	0.280	5310	Buck et.al., 2007
[e]K-ECF	GF	0.125	0.280	651	Davies and Morris 1993, and Buck et.al., 2007
[ef]GF	Tubular	0.125	0.00480	37500	Davies and Morris 1993, McNamara et al., 2008
Bladder	Urine	0.000972	0.30	4.67	Davies and Morris 1993, Lukacz et al., 2011

[a]Arterial blood & [v]venous

[b]Transfer rate (day^{-1}) was computed by (flow rate(L/Min) x 24 x 60)/ (Volume of source(L))

[c]Flow rate and volume of source compartment for the ROB were computed using the concept of mass balance

[d]Renal blood flow rate of 1L/Min was used while calculating transfer rate

[e]Glomerular filtration rate was used as a flow rate

[f]The total volume of all glomeruli in the kidneys was used as the volume of source compartment

Table 5. Transfer Rates Values for Model-B

Blood distributions transfer rates in the humans (Model-B)					
Source Compartment	Target Compartment	Flow rate (L/Min)	Volume of source compartment (L)	Transfer rate (day^{-1}) [b]	Reference
[v]Plasma	Lung	6.08	4.42	1980	De Buck et.al., 2007
[a]Lung	Plasma	6.08	1.11	7890	De Buck et.al., 2007
[c]ROB	Plasma	4.95	76.12	93.6	Total Blood flow and total volume obtained from Buck et.al., 2007
[a]Plasma	ROB	6.08	2.21	3960	De Buck et.al., 2007
[ad]Plasma	K-ECF	1.00	2.21	651	Douglas and Pooler 2016
Kidney-ECF	Plasma	1.02	0.28	5310	Buck et.al., 2007
[e]K-ECF	Bladder	0.125	0.28	651	De Buck et.al., 2007
Bladder	Urine	0.000972	0.30	4.67	Davies and Morris 1993, Lukacz et al., 2011

[a]Aarterial blood & [v]venous

[b]Transfer rate (day-1) was computed by (flow rate(L/Min) x 24 x 60)/ (Volume of source(L))

[c]Flow rate and volume of source compartment was computed using the concept of mass balance

[d]Renal blood flow rate of 1 L/min was used while calculating transfer rate

[e]Glomerular filtration rate was used as flow rate

Table 6. Parameters used in SAAM-II for Model-A

Parameters for model-A					
Source Compartment	Target Compartment	Transfer Rate (ID)	Transfer rate (day^{-1})	Reference	Fixed/Fitted
Plasma	Lung	6,1	1980	Table 4	Fixed
Lung	Plasma	1,6	7890	Table 4	Fixed
ROB	Plasma	1,5	91.4	Table 4	Fixed
Plasma	ROB	5,1	3960	Table 4	Fixed
Plasma	K-ECF	2,1	652	Table 4	Fixed
K-ECF	Plasma	1,2	5310	Table 4	Fixed
K-ECF	GF	7,2	651	Table 4	Fixed
K-ECF	Tubular	3,2	Adjustable	-	Fitted
Tubular	K-ECF	2,3	Adjustable	-	Fitted
Tubular	Bladder	4,3	Adjustable	-	Fitted
GF	Tubular	3,7	37500	Table 4	Fixed
Bladder	Tubular	3,4	0	-	Fixed
Bladder	Urine	8,4	4.67	Table 4	Fixed

Table 7. Parameters used in SAAM II for Model-B

Parameter for model-B					
Source Compartment	Target Compartment	Transfer Rate (ID)	Transfer rate (day^{-1})	Reference	Fixed/Fitted
Plasma	Lung	6,1	1980	Table 5	Fixed
Lung	Plasma	1,6	7890	Table 5	Fixed
ROB	Plasma	1,5	93.6	Table 5	Fixed
Plasma	ROB	5,1	3960	Table 5	Fixed
Plasma	K-ECF	2,1	651	Table 5	Fixed
K-ECF	Plasma	1,2	5310	Table 5	Fixed
K-ECF	Bladder	3,2	651	Table 5	Fixed
Bladder	K-ECF	2,3	0	-	Fixed
Bladder	Urine	4,3	4.67	Table 5	Fixed

Table 8. Transfer Rate Values for Model-A

Transfer rates (model-A)		
Source Compartment	Target Compartment	Transfer rate (day^{-1})
Plasma	Lung	1980
Lung	Plasma	7890
ROB	Plasma	91.4
Plasma	ROB	3960
Plasma	K-ECF	652
K-ECF	Plasma	5310
K-ECF	GF	651
K-ECF	Tubular	19.8
Tubular	K-ECF	151
Tubular	Bladder	50.0
GF	Tubular	37500
Bladder	Tubular	0.0
Bladder	Urine	4.7

Table 9. Statistical Parameters for Various Models

Total sample size >40							
Model Type	AIC_{SAAM}	Sample Size (N)	$AIC_{LITERATURE}$	ΔAIC	Relative Likelihood	Akaike Weight	Ranking
Model-A	1.73	77.0	267	0.00	$1.00x10^{0}$	1.00×10^{0}	1st
Model-B	1.85	77.0	285	17.9	1.30×10^{-04}	1.30×10^{-04}	2nd
Giussani Model	4.79	77.0	738	471	*	*	3rd
ICRP model	5.75	77.0	885	618	*	*	4th
Total Relative Likelihood						1.00×10^{0}	
Total Akaike Weight						1.00×10^{0}	

* = insignificantly small

Based on the AIC values (Table 9), the model-A, and the ICRP model were found to be the most favorable, and the least favorable model, respectively. The Akaike weight of model-A was found to be unity signaling that it was 100% plausible compared relatively to other models of interest for a given data set. The Akaike weight values of all models sum to unity, which suggests that the calculations were performed appropriately.

Four graphs, developed using the data obtained from the Figure 16, demonstrate the percentage of whole-body retention against the time after incorporation. There are for each model evaluated Figure 20, 21, 22, and 23 for model A, and model-B, the Giussani model, and the ICRP model, respectively. Likewise, four more graphs, developed using the data from the Figure 17, of the daily urine excretion per day against the time after incorporation were also plotted using SAAM II software. These graphs are produced in Figure 24, 25, 26, and 27 for model-A, the model-B, the Giussani model, and the ICRP model, respectively. Based on visual inspections of these graphs, model-A was found to be the most favorable one. As such, the model-B, the Giussani model, and the ICRP models were subjectively found to not fit the whole-body retention and urine excretion data well. Likewise, from the visual inspections of the graphs, the ICRP model was found to be the least favorable of the four, and seems to over fit the data.

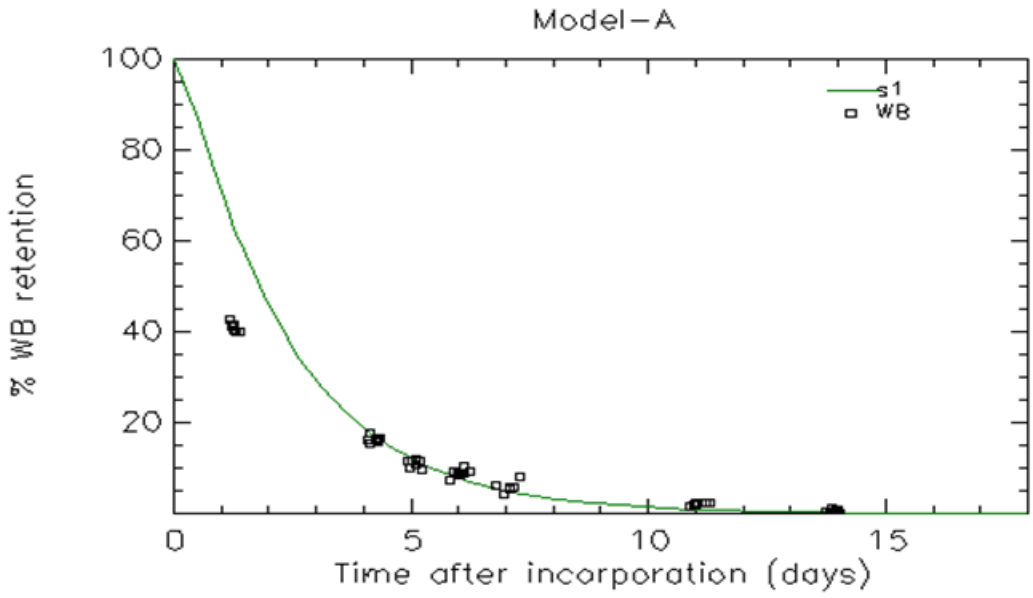

Figure 20. % WB retention vs time for Model-A Mo model

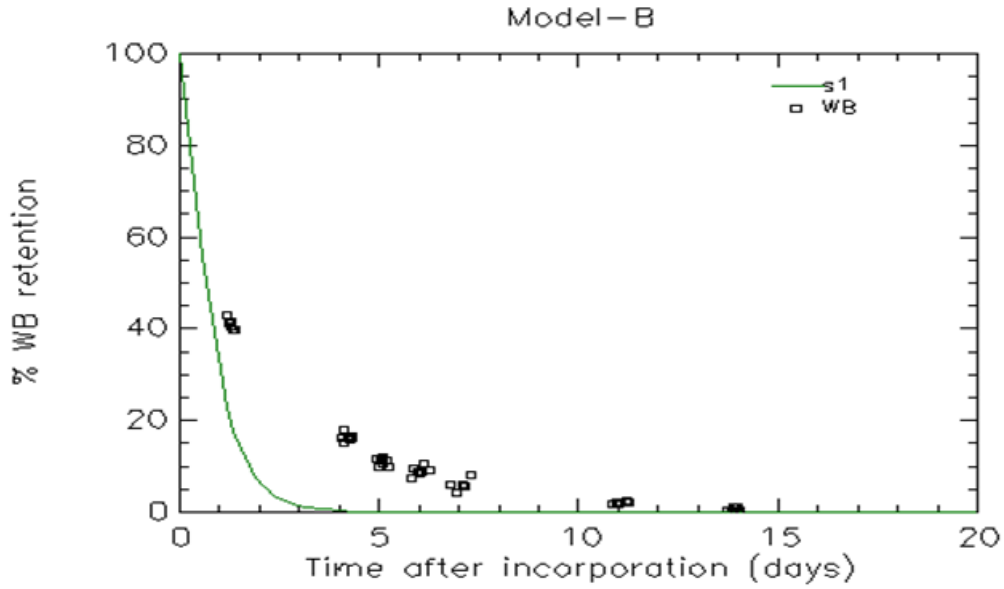

Figure 21. % WB retention vs time for Model-B Mo model

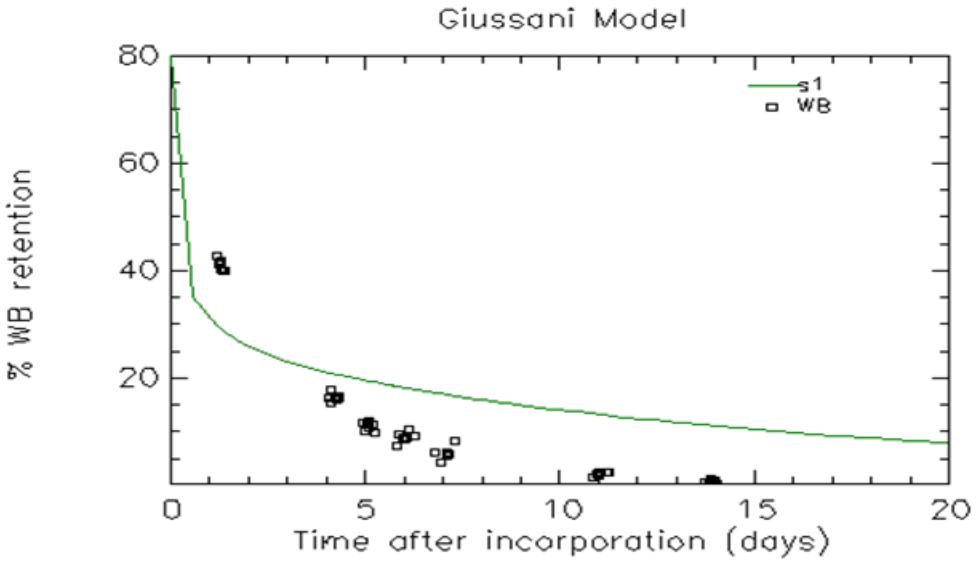

Figure 22. % WB retention vs time for Giussani Mo model

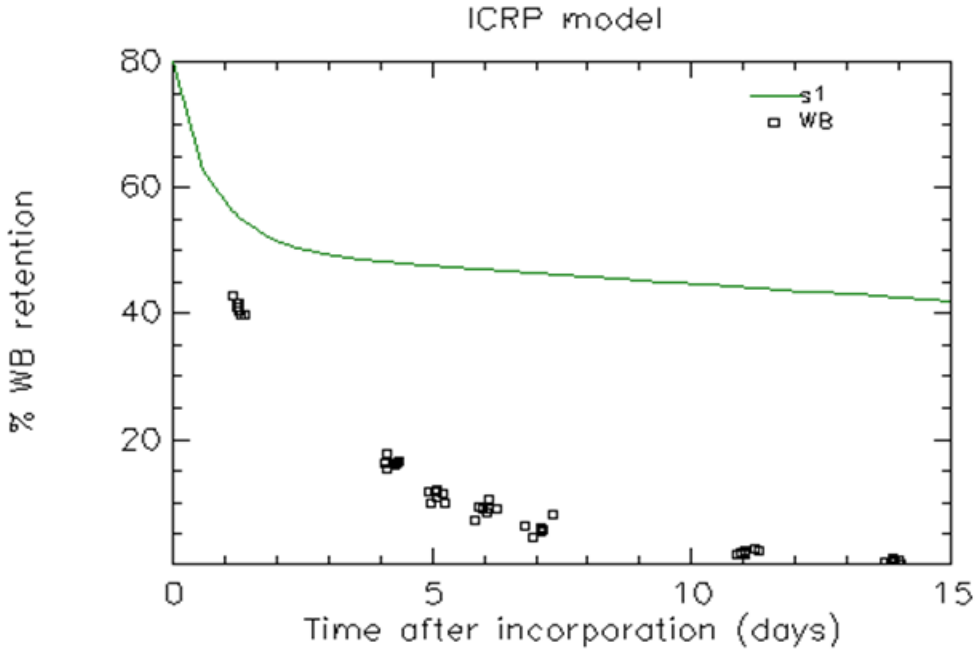

Figure 23. % WB retention vs time for ICRP Mo model

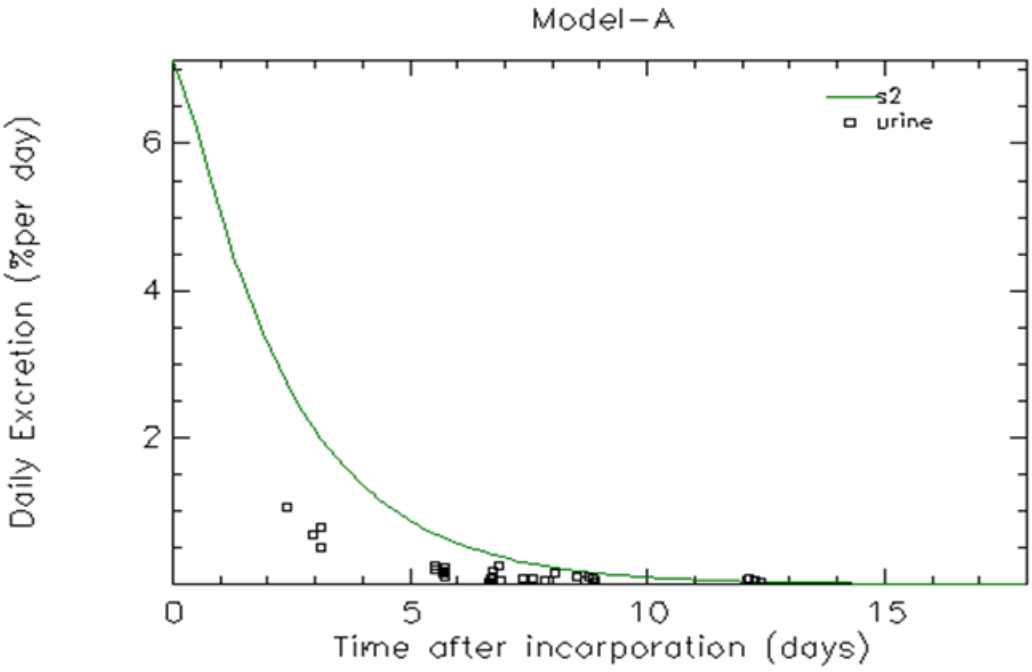

Figure 24. Daily excretion % per day Vs time for model-A Mo model

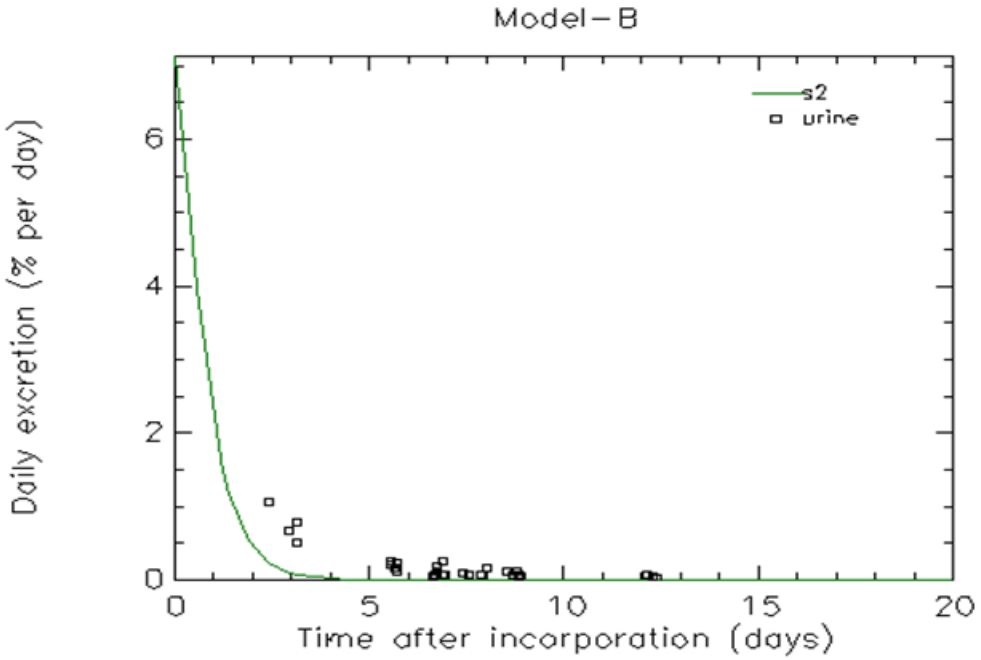

Figure 25. Daily excretion % per day Vs time for model-B Mo model

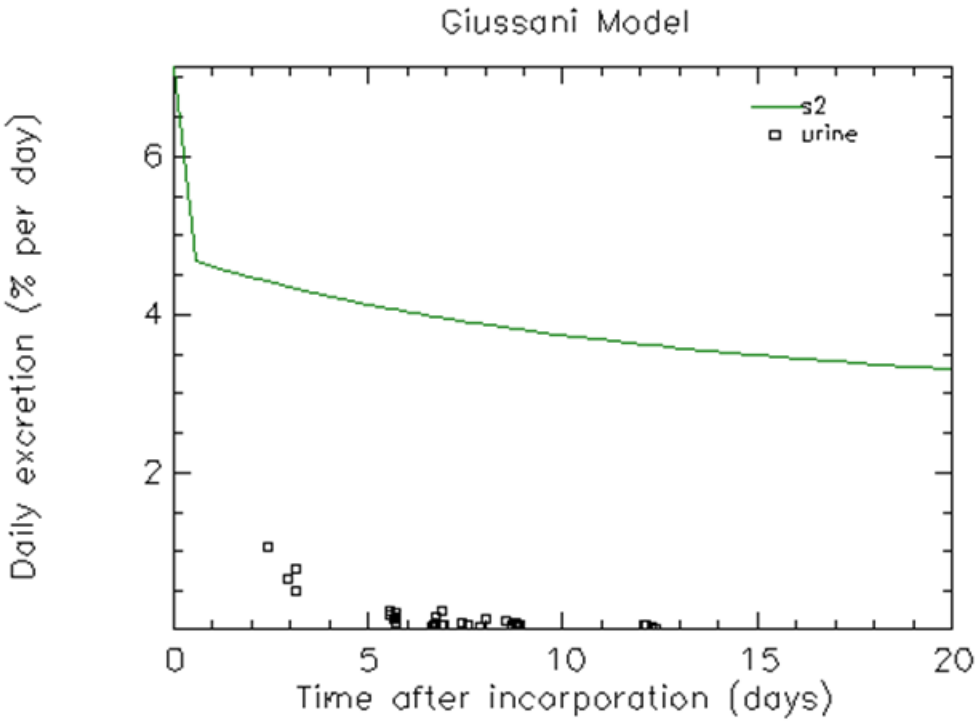

Figure 26. Daily excretion % per day Vs time for Giussani model Mo model

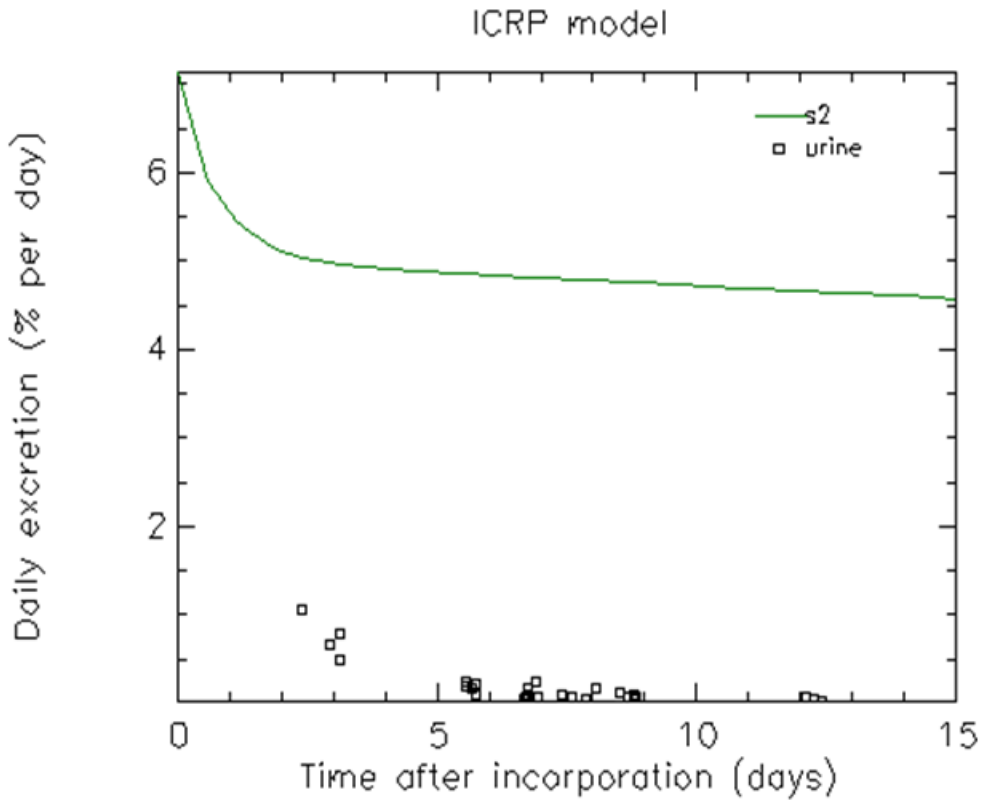

Figure 27. Daily excretion % per day Vs time for ICRP Mo model

It was also concluded from Figure 23, and 27 that the ICPR model over-predicts the WB retention, and excretion data. Likewise, it was also concluded that from Figure 20, and 24 that model-A neither over-predicts nor under-predicts the dataset used in this project. Absorbed internal dose is a product of the number of transformations occurring per organ and the energy deposited per transformation. Model-A with more accurate transfer rate will have a more accurate estimate number of the transformations occurring in an organ. The energy imparted for a given radionuclide remains unchanged for a given radionuclide as it is based on factors independent of biokinetics. Consequently, model-A, with the better transfer rates values providing a better fit to excretion information and consequently an assumed better fit of retention, probably can estimate dose for molybdenum radionuclides more accurately.

Based on visual inspections of the graphs (Figures 20-28), the AIC values, and the Akaike weight values, it was found that the ICRP model was the least favorable model, and the model-A was found to be more accurate. Therefore, it was concluded that the revision of the ICRP Mo biokinetic model may be necessary to better predict the Mo exposure in humans.

4.3 Hypothesis Testing and Discussions

Two hypotheses which were tested in this project are listed below.

$H_{0,1}$: Most of the molybdenum excretion in the kidney is predominantly a function of glomerular filtration.

$H_{A,1}$: Most of the molybdenum excretion in the kidney is not predominantly a function of glomerular filtration.

$H_{0,2}$: Molybdenum excretion in the kidney follows linear kinetics.

$H_{A,2}$: Molybdenum excretion in the kidney does not follows linear kinetics.

Decision rule: The model associated with the lower AIC score is considered more probable.

There was a strong evidence based on the lower AIC values that model-A would best fit new data relative to the other models. Therefore, it was deduced that the first, and the second alternative hypotheses were more favorable. It was observed that not only does glomerular filtration play an important role in molybdenum filtration, but also tubular secretion and tubular re-absorption apparently play mathematically important roles in the describing filtration. Likewise, it was also concluded that molybdenum excretion in the kidney does not favor a linear kinetics.

Literature values of granular filtration rates are available in the literature (described in section 2.6.1.1). Tubular secretion and tubular re-absorption values for molybdenum kidney filtration were obtained empirically. It would be necessary to directly measure filtration in vivo to understand these values by means of fundamentals measurements. A procedure to do such measurement has not thus far been found in the literature.

CHAPTER 5. CONCLUSIONS

The objective of this research was to develop a physiologically based model using the PBPK modeling approach for molybdenum in order to better define and understand the physiological relevance of kidney transfer rates in humans. The PBPK based model-A, and model-B, were proposed in this project. The values of transfer rates were obtained by measured kinetics of mechanisms if possible. Three out of thirteen transfer rates needed in model-A required empirical fitting. However, for model B, no empirical fitting was required. The SAAM II software was used to quantitatively evaluate the quality of the model. The SAAM II is widely regarded as the most robust and accurate package for solving systems of differential equations and for fitting model parameters to experimental data sets with specified error models. The statistical concept of AIC was used to find the goodness of fit. The AIC values were obtained from the SAAM II software and were used to evaluate the model fits. The ICRP model and the Giussani model were reconstructed in SAAM II using their respective published transfer coefficient values.

There was strong evidence that model-A would best fit new data relative to the other models. Therefore, it was concluded that the first, and the second alternative hypotheses were more favorable. It was concluded that not only does glomerular filtration plays a role in molybdenum filtration, but also tubular secretion and tubular reabsorption apparently plays mathematically important roles in molybdenum filtration. Likewise, it was also concluded that molybdenum excretion in the kidney does not favor a linear kinetics.

It was also concluded that the ICRP model over-predicts the WB retention, and daily excretion data. Likewise, it was also concluded that that model-A neither over-predicts nor under-predicts the WB retention and urinary excretion data. Absorbed internal dose is a product of the number of transformations occurring per organ and the energy deposited per transformation.

Model-A with more accurate transfer rate will have a more accurate estimate number of the transformations occurring in an organ. The energy imparted for a given radionuclide remains unchanged for a given radionuclide as it is based on factors independent of biokinetics. Consequently, model-A, with the better transfer rates values providing a better fit to excretion information and consequently an assumed better fit of retention, probably can estimate dose for molybdenum radionuclides more accurately.

Based on visual inspection of the various graphs (percent retention vs time, and percentage daily excretion per day vs time), the AIC values, and the Akaike weight values, it was concluded that the ICRP model was the least favorable model, and the model-A produced the best fit of the data. The improved model can provide more accurate estimates of the internal dose for molybdenum radionuclides. Therefore, it was concluded that the revision of the ICRP molybdenum biokinetic model may be necessary to better predict the molybdenum exposure in humans more accurately

CHAPTER 6. FUTURE DIRECTIONS

The data used in this project were obtained as a result of accidentally inhaled ^{99}Mo and ^{99m}Tc by a group of seven workers belonging to ^{99m}Tc manufacturing generators for use in nuclear medicine. The first measurements were performed 1.3 days after the accident happened. Since molybdenum excretion mostly occurs via urine within first 24 hours, it would be better to test the newly constructed best model-A with the immediately collected data in the near future. However, this is a challenging task because similar accident may not occur in an occupational setting.

It was observed that not only does glomerular filtration play an important role in molybdenum filtration, but also tubular secretion and tubular re-absorption apparently play mathematically important roles in molybdenum filtration. GFR values were found easily in the literature, however tubular secretion and tubular re-absorption values for molybdenum kidney filtration were difficult to find. It would be necessary to directly measure filtration in vivo to understand these values by means of fundamentals measurements.

Validity of the proposed models in this project can be tested by using another type of statistical resampling technique called Leave-one-out cross validation. It may not even be required, since Stone 1977 showed that the AIC and leave-one-out cross validations are asymptotically equivalent. Nonetheless, one may perform it in the future to get the same experience M. Stone did in 1977.

CITATIONS

[1] Abumrad N. Naji. Molybdenum-Is It an Essential Trace Metal? New York Academy of Medicine. Vol 60. No-2; 1984

[2] Allaway W.H, Kubota Joe, Losee Fred. Selenium. Molybdenum, and vanadium in Human Blood. Archives of Environmental Health: An International Journal. Volume 16, Issue-3; 1968.

[3] Alvarez A., Navarro N., Salvador S. Urinary Excretion Measurement After Accidental Inhalation of 99mTc and 99Mo. Radiation Protection Dosimetry, Vol. 50, No.1, pp,59-61; 1994.

[4] Arrington L.R. and Davis G.K. Molybdenum toxicity in the rabbit. J. Nutr. 51, 295–304; 1953.

[5] Bohle A, Aeikens B, Eenboom A, Fronholt L., Rudiger W., xiao J., Greschniok A., Wehrmann M. Human glomerular structure under normal conditions and in isolated glomerular disease. *Kidney Int Suppl*.1998; 67: S186-S188. doi:10.1046/j.1523-1755; 1998

[6] Brewer GJ, Askari F, Dick RB, Sitterly J, Fink JK, Carlson M, Kluin KJ, Lorincz MT. Treatment of Wilson's disease with tetrathiomolybdate: V. Control of free copper by tetrathiomolybdate and a comparison with trientine. TranslRes, 154:70–7: 2009.

[7] Burnham, K., and Anderson, D. Model Selection and Multimodel Inference: A Practical Information-Theoretic Approach. 2nd ed., Springer-Verlag New York Inc.; 2002.

[8] Cao Y, Balthasar JP, Jusko WJ. Second-generation minimal physiologically-based pharmacokinetic model for monoclonal antibodies. J Pharmacokinetic Pharmacodynamic Vol.40 (5):597–607; 2013.

[9] Capogni Marco, Pietropaolo Antonino, Quintieri Lina, Angelone Maurizio, Boschi Alessandra. 14 Mev Neutrons for 99Mo/99mTc Production: Experiments, Simulations and Perspectives. Molecules, doi: 10.3390/molecules23081872; 2018.

[10] CDC (Centers for Disease Control and Prevention). The National Institute for Occupational Safety and Health (NIOSH). Accessed on June 8th, 2021. Available at. https://www.cdc.gov/niosh/npg/npgd0433.html.2021.

[11] Clark H. Leona, Setzer R. Woodrow, Barton A. Hugh. Framework for Evaluation of Physiologically-based Pharmacokinetic Models for Use in Safety or Risk Assessment. Risk Analysis, Vol.24, No.6; 2004.

[12] Davies Brian, Morris Tim. Physiological Parameter in Laboratory Animals and Humans. Pharmaceutical Research. Vol. 10, No. 7, P-1093-1095; 1993.

[13] De Buck S. Stefan. Sinha K. Vikash, Fenu A. Luca and Nijsen Marjoleen. Prediction of Human Pharmacokinetics Using Physiologically Based Modeling: A Retrospective Analysis of 26 Clinically Tested Drugs. Drug Metabolism and Disposition 35(10):1766-80. Published on PubMed; 2007.

[14] Department of State Health Services, Texas. What you should know about molybdenum. Accessed on November 2, 2020 Available at https://www.dshs.texas.gov/epitox/educational/molybdenum.doc; 2012

[15 Desai B. Babasaheb. Handbook of Nutrition and Diet. Marcel Dekker, Inc. Basel, NY, C-7, 0-148; 2000.

[16] Disler B. P, Lynch R. S, Charlton W. R, Torrance D. J, Bothwell H. T, Mayet F. The effect of tea on iron absorption. Gut. Vol.16 (3): 193-200; 1975.

[17] Doerfel H., Andrasi A, Bailey M, Berkovski V, Blanchardon E, Castelani M, Cruz-Suarez R, Etherington G, Hurgten C, LeGuen B, Malatova I, Marsh J, Stather J. "The science and art of internal dose assessment." Internal Dosimetry. International Radiation Protection Association; 2002.

[18] Douglas C. Eaton, Pooler P. John. Renal Blood Flow and Glomerular Filtration. “Vander’s Renal Physiology. Accessed on August 24, 2020. Available on http://accessmedicine.mhmedical.com/content.aspx?bookid=2173&sectionid=163663126#:~:text=Renal%20blood%20flow%20(RBF)%20is,its%20total%20volume%20every%20minute.; 2016.

[19] EPA (Environmental Protection Agency). EPA Facts about Technetium-99. Accessed on May 11 2020. Available on https://www.nrc.gov/docs/ML1603/ML16032A152.pdf; 2002.

[20] EPA (Environmental Protection Agency). Physiologically-Based Pharmacokinetic (PBPK) models. Scientific Models to Help Evaluate Health Effects of Chemical. Science in Action. Innovative Research for A Sustainable Future. EPA Office of the Research and Development: 2018.

[21] EPA (Environmental protection Agency). Radiation Protection. Radionuclide Basics: Technetium-99. Accessed on May 11 2020. Available on https://www.epa.gov/radiation/radionuclide-basics-technetium-99; 2017.

[22] European Commission. Health & Consumer Protection Directorate-General. Scientific Committee on Food. Opinion of the scientific committee on Food on the Tolerable Upper Intake Level of Molybdenum. Accessed on May 5th 2020. Available at https://ec.europa.eu/food/sites/food/files/safety/docs/sci-com_scf_out80h_en.pdf; 2000.

[23] Fairhall L.T., Dunn R.C.,Sharpless N.E. and Pritchard E.A., The Toxicity of Molybdenum, Public Health Bull. No. 293. US Government Printing Office, New York; 1945.

[24] Gharehbaghi Maysam, Shemirani Farzaneh. Ionic liquid based dispersive liquid micro extraction and enhanced spectrophotometric determination of Mo (VI) in water and plant leave samples by FO- LADS, Food and Chemical Toxicology 49; 2011.

[25] Giussani Augusto, Arogunjo M. Adeseye, Cantone C. Marie, Tavola Federico, Veronese Ivan. Rates of intestinal absorption of molybdenum in humans. Applied Radiation and Isotopes. Volume 64, P -639-644; 2006.

[26] Giussani Augusto, Cantone Marie, Hollriegl Vera, Oeh Uwe, Tavola Federico, Ivan Veronese. Modeling Urinary Excretion of Molybdenum after Oral and Intravenous administration of stable. Radiation Protection Dosimetry. Vol.127, No. 1-4, pp.136-139; 2007.

[27] Giussani, A., Cantone, M.C., Tavola, F, Veronese I, Lopez A. M, Navarro T. 2004. Validation of the Revised Model for the Biokinetics of Molybdenum with Data from a Real Accidental Case. 11th International Congress of the International Radiation Protection Association IRPA-11, 23; 2004.

[28] ICRP (International Commission on radiological Protection). Limits for Intakes of Radionuclides by workers. ICRP publication 30, part 1. Volume 2, No. ¾, P (83-85); 1979.

[29] ICRP (International Commission on radiological Protection). Occupational; intakes of radionuclides: part 2. ICRP publication 134. Ann. ICRP 45(3/4), 1-352; 2016.

[30] IOMA (International Molybdenum Association. History of Molybdenum. Accessed May 4, 2020. Available at: http://www.imoa.info/molybdenum/molybdenum-history.php: 2020.

[31] Jones HM, Rowland Yeo K. Basics Concepts in Physiologically Based Pharmacokinetic Modelling in Drug Discovery and Development. COT: CPT Pharmacometrics & systems pharmacology; 2013.

[32] Speight G. James. Properties of inorganic compounds. Environmental Inorganic Chemistry for Engineers. P-171-229; 2017

[33] Kselikova Marie, Marik Tomas, Lener Jaroslav. Interaction of molybdenum with human erythrocytes membrane proteins. Biological Trace Element research. Accessed on May 7, 2020. Available at https://link.springer.com/article/10.1007/BF02789035; 1980.

[34] Kuepfer L. Niederalt C, Wendl T, Schlender J-F, Willmann S, Lipppert J, Block M, Eissing T, Teutonico D. Applied Concepts in PBPK Modeling: How to Build a PBPK/PD Model. CPT Pharmacometrics & systems pharmacology; 2016.

[35] Lenntech. Water Treatment Solution: Molybdenum. Accessed 3 May 2020. Available at: http://www.lenntech.com/periodic/elements/mo.htm; 2020.

[36] Lobbi-Nivol Chantal, Leimkuhler Silke. Molybdenum enzymes, their maturation and molybdenum cofactor biosynthesis in Escherichia coli. ScienceDirect. ELSEVIER. Vol-1827 pp 1086-1101; 2013.

[37] Lukacz, E. S., Sampselle, C., Gray, M., Macdiarmid, S., Rosenberg, M., Ellsworth, P., & Palmer, M. H. A healthy bladder: a consensus statement. *International journal of clinical practice*, *65*(10), 1026–1036; 2011.

[38] Marangoni A. Alejandro. Enzyme Kinetics. A Modern Approach. Published by John Wiley & Sons, Inc., Hoboken, NJ; 2003.

[39] Maret Wolfgang, Wedd Anthony. Binding, Transport and storage of Metals Ions in Biological Cells. Published by the Royal Society of Chemistry. RSC Metallobiology series No.2.Cambridge, UK; 2014.

[40] Mayo Clinic. Wilson's disease. Accessed on May 4th 2020. Available at https://www.mayoclinic.org/diseases-conditions/wilsons-disease/symptoms-causes/syc-20353251; 2020.

[41] Mclaughlin PD, Jones B., Maher M. An update on radioactive release and exposures after Fukushima Dai-ichi disaster. National Center for Biotechnology Information, U.S. National Library of Medicine. Br J Radiol. PMCID: PMC3487052; 2012.

[42] McNamara, B. J., Diouf, B., Hughson, M. D., Douglas-Denton, R. N., Hoy, W. E., & Bertram, J. F. Renal pathology, glomerular number and volume in a West African urban community; 2008.

[43] Medium. Towards data Science. Information to AIC-Akaike Information Criterion. Accesses on June 6th 2020. Available at https://towardsdatascience.com/introduction-to-aic-akaike-information-criterion-9c9ba1c96ced#:~:text=In%20plain%20words%2C%20AIC%20is,lower%20AIC%20score%20is%20better; 2020.

[44] Mendel R. Ralf, Kruse Tobias. Cell biology of molybdenum in plants and humans. Biochimica et Biphysica Acta. Vol-1823, pp (1868-1579; 2012.

[45] Mendel R. Ralf. The Molybdenum Cofactor. JBC Papers Press. Journal of Biological Chemistry. V-288. Number 19; 2013.

[46] Pillai R.A. Maroor, Dash Ashutosh, and Knapp F.F. Jr. Sustained Availability of 99mTc: Possible Paths Forward. Journal of Nuclear Medicine. Doi 10.2967/jnumed.110338; 2012.

[47] Mills CF, Brenner I. Nutritional aspects of molybdenum in animals. Molybdenum and molybdenum containing enzymes. Oxford: Pergamum; 1980.

[48] Mills CF, Davis GK, Molybdenum. In: Mertz W. ed. Trace elements in human and animal nutrition. 5th ed. San Diego: Academic Press: 429-63; 1987.

[49] National Center for Biotechnology Information (NCBI). Molybdenum-99 for Medical Imaging. Accessed on May 11 2020. Available on https://www.ncbi.nlm.nih.gov/books/NBK396163/; 2016.

[50] National Institute of Diabetes and Digestive and Kidney Diseases (NIH).Your Kidneys and How They work. Accessed on June 6, 2020. Available on https://www.niddk.nih.gov/health-information/kidney-disease/kidneys-how-they-work: 2020.

[51] National Institute of Health (NIH). U.S. National Library of Medicine. Environmental health and Toxicology Information. Disposition Models. Accessed on May 26 2020. Available at ht. tps://toxtutor.nlm.nih.gov/11-003.html; 2020.

[52] National Institutes of Health (NIH): Molybdenum: Accessed on May 4, 2020. Available at: https://ods.od.nih.gov/factsheets/Molybdenum-HealthProfessional/; 2020.

[53] NJ Health (2011). Department of Health. Hazardous Substance Fact Sheet. Molybdenum. Accessed on June 7th, 2021. Available at https://nj.gov/health/eoh/rtkweb/documents/fs/1309.pdf; 2021.

[54] Nordberg. F. Gunnar, Fowler A. Bruce, Nordberg Monica, Friberg T. Lars. Handbook on the Toxicology of Metals. Copyright at Elsevier B.V. Third Edition. Chapter 34, p (731-739): 2007.

[55] Novotny A Janet, and Peterson A. Catherine: Molybdenum. Oxford Academics, Advances in nutrition, Volume 9, Issue 32018, 9, 272-273; 2018.

[56] Washington State Department of health. Technetium-99m, Fact Sheet. Division of Environmental Health Office of Radiation Protection. Accessed on June 2021. Available at https://www.doh.wa.gov/portals/1/Documents/Pubs/320-083_tc99_fs.pdf; 2012.

[57] Poudel Deepesh. Systematic and wound behavior of ^{238}Pu IV citrate in nonhuman primates. PhD. dissertation. Idaho State University library; 2016.

[58] Preston Alexandra. Nutritional Biochemistry Explained. Distributed by Lulu at www.lulu.com. First Edition. P (29-30); 2014.

[59] Rajagopalan KV. Molybdenum-An Essential Trace Element. Accessed on August 20, 2020. Available at https://doi.org/10.1111/j.1753-4887.1987.tb00981.x; 1987.

[60] Riviere E. Jim. Basic Principles and Techniques of Pharmacokinetic modeling. Journal of Zoo and Wildlife Medicine 28(1): 3-19; 1997.

[61] Sardesai M. Vishwanath. An Essential Trace Elements. Nutrition in Clinical Practice. Vol.8, PP (277-281); 1993.

[62] Scanlon C. Valerie, Sanders Tina. Essentials of Anatomy and Physiology. Fifth Edition. Published by F.A. Davis Company. Chapter (18). P (417-428); 2007.

[63] SHINE (2021). Health, Illuminated! Accessed on June 7th, 2021. Available at https://shinemed.com/mo-99/. Statisticshowto ; 2020.

[64] Shampine L.F. Implementation of Rosenbrock Methods. ALS Transactions on Mathematical Software, col 8, No 2; 1982.

[65] Statistics for the rest of us! Accessed on June 6th 2020. Available at https://www.statisticshowto.com/contact/; 2020.

[66] Stone M. An Asymptotic Equivalence of Choice of Model by Cross-validation and Akaike's Criterion. Journal of the Royal Statistical Society. Series B (Methodological), Volume 39, Issue 1, 44-77; 1977.

[67] Tejada-Jimenez Manuel, galvan Aurora, and Fernandez Emilo. Algae and humans share a molybdate transporter. PNAS, Vol. 108. No. 16; 2011.

[68] The Epsilon Group (TEG). Driven by Modelling. Software. SAAM II. Accessed on May 31 2020. Available on https://tegvirginia.com/software/saam-ii/; 2020.

[69] Thompson H. Katherine, Turnlund R. Judit. Kinetic Model of Molybdenum Metabolism Developed from Dual Stable Isotope Excretion in Men Consuming a Low Molybdenum Diet. The Journal of Nutrition, Volume 126, Issue 4, P (693-972); 1996.

[70] Turnlund R. Judith, Keyes R. William, and Peiffer L. Gary. Molybdenum absorption. Excretion, and retention studied with stable isotopes in young men at five intakes of dietary molybdenum. Am J Clin Nutr. American Society for clinical Nutrition; 1995.

[71] Turnlund R. Judith, Keyes R. William. Plasma molybdenum reflects dietary molybdenum intake. Journal of Nutritional Biochemistry; 2004.

[72] Versieck, J., Hoste, J, Barbier,F. Vaballenberghe, L. de Rudder, J.& Cornelis,R. Determination of molybdenum in human serum by neutron activation analysis. Clin. Cjim. Acta 87: 135-140; 1978.

[73] Voropanova. L.A, Barvinyuk N.G, Extraction of molybdenum (VI) from aqueous peroxide solutions of sodium tungstate with trialkylamine, Russ. J. Appl. Chem; 2004.

[74] Vyskocil Adolf, Viau Claude. Assessment of Molybdenum Toxicity in Humans. Journal of Applied Toxicology. J. Appl. Tocicol; 1999.

[75] Walravens P.A., Moure-Eraso R., Solomons C.C., Chapell W.R. and Bentley G. Biochemical abnormalities in workers exposed to molybdenum dust. Arch. Environ. Health 34; 1979

Appendix 1.1 Data Extrapolated from Figure 15

Time after incorporation (days)	Daily excretion (% per day)
2.391	1.051
3.132	0.787
2.947	0.665
3.131	0.502
5.543	0.243
5.728	0.227
5.542	0.206
5.682	0.169
5.681	0.16
5.727	0.106
6.887	0.253
6.748	0.18
6.747	0.106
6.702	0.079
6.934	0.063
6.656	0.037
7.397	0.09
7.583	0.079
7.861	0.058
8.046	0.158
8.51	0.111
8.788	0.106
8.833	0.079
8.695	0.063
8.834	0.037
12.126	0.079
12.265	0.053
12.404	0.021

Appendix 1.2 Data Extrapolated from Figure 16

Time after incorporation (days)	% WB retention	Time after incorporation (days)	% WB retention
1.166	42.866	6.093	10.489
1.218	41.042	6.092	8.893
1.219	41.498	6.252	9.121
1.272	40.358	6.781	6.156
1.271	41.726	6.940	4.332
1.325	39.902	7.097	5.472
1.377	39.902	7.098	5.628
4.079	16.188	7.099	5.928
4.132	17.785	7.152	5.700
4.131	15.272	7.311	8.208
4.238	16.189	10.861	1.596
4.291	15.961	10.967	2.052
4.310	16.189	11.010	2.052
4.344	16.645	11.020	1.824
4.927	11.629	11.021	2.279
4.980	10.033	11.232	2.508
5.033	11.629	11.285	2.280
5.085	10.717	13.722	0.455
5.086	12.085	13.828	0.456
5.192	11.401	13.881	1.140
5.245	9.805	13.880	0.456
5.828	7.296	13.934	0.912
5.881	9.349	13.987	0.912
5.987	8.893	14.040	0.228
6.040	8.436		

Appendix 2.1 AIC in SAAM II

$AIC_{SAAM} = \frac{L+Np}{M}$

Where,

- Np is the number of adjustable parameters in the model (plus the number of variance parameters if relative weights are considered)
- L is calculated from the objective function R(p), which is minimized to produce the best fitting model;

$$L = \left(\frac{M}{2}\right)(R(P) + ln(2\pi))$$

- M is the total number of data points
- $AIC_{Literature} = AIC_{SAAM} * 2M = \frac{L+Np}{M} * 2M$
- Hence, AIC = 2L+2Np

Appendix 2.2 Software used (SAAM II)

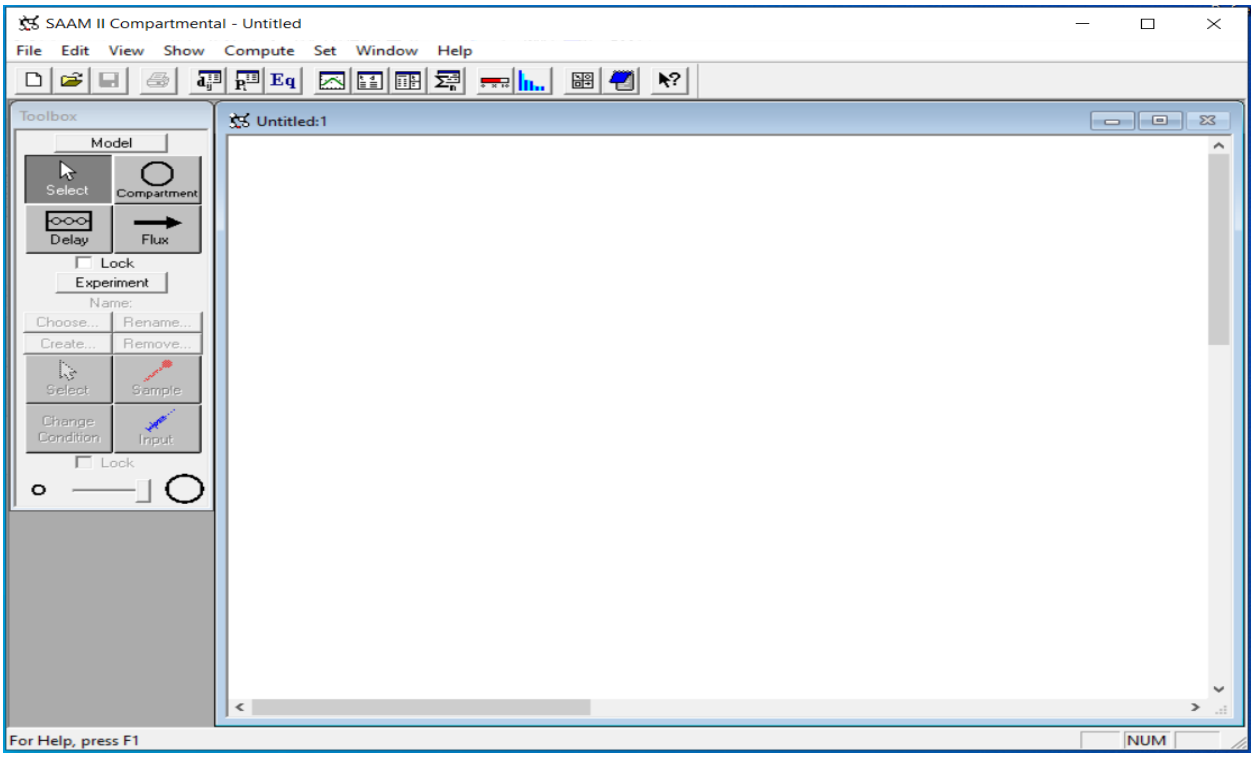

Appendix 2.3 SAAM II input data for Model-A

Equations

```
Equations Defined Elsewhere (read-only):

flux(3,7) = k(3,7) * q7
flux(7,2) = k(7,2) * q2
flux(3,4) = k(3,4) * q4
flux(8,4) = k(8,4) * q4
flux(6,1) = k(6,1) * q1
flux(1,6) = k(1,6) * q6
flux(1,2) = k(1,2) * q2
flux(2,1) = k(2,1) * q1
flux(3,2) = k(3,2) * q2
flux(2,3) = k(2,3) * q3
flux(4,3) = k(4,3) * q3
flux(5,1) = k(5,1) * q1
flux(1,5) = k(1,5) * q5
ex1.bolus = 0.0
ex1.infusion = 0.0
s2 = (100-q8)/14.0182
s1 = q1+q2+q3+q4+q5+q6+q7
```

AIC and BIC values

	Objective	Scaled Data Variance
s2 : urine	-3.127938e-001	9.893383e+002
s1 : WB	1.811697e+000	1.598868e+001

Total objective	1.498903e+000	
AIC	1.733325e+000	
BIC	1.809423e+000	

Appendix 2.4 SAAM II input data for Model-B

Equations

```
Equations Defined Elsewhere (read-only):

flux(6,1) = k(6,1) * q1
flux(1,6) = k(1,6) * q6
flux(1,2) = k(1,2) * q2
flux(2,1) = k(2,1) * q1
flux(3,2) = k(3,2) * q2
flux(2,3) = k(2,3) * q3
flux(4,3) = k(4,3) * q3
flux(5,1) = k(5,1) * q1
flux(1,5) = k(1,5) * q5
ex1.bolus = 0.0
ex1.infusion = 0.0
s2 = (100-q4)/14.0182
s1 = q2+q5+q1+q6+q3
```

AIC and BIC values in SAAM

```
                          Objective      Scaled Data Variance
s2 : urine              -1.147806e+000       9.693935e+001
s1 : WB                  2.930486e+000       9.031553e+001
                        --------------
Total objective          1.782680e+000

AIC                      1.849240e+000
BIC                      1.894898e+000
```

Appendix 2.5 AIC from SAAM for Giussani Model

	Objective	Scaled Data Variance
s2 : urine	1.789980e+000	3.126985e+005
s1 : WB	5.879265e+000	9.293830e+003

Total objective	7.669245e+000	
AIC	4.792522e+000	
BIC	4.838181e+000	

Appendix 2.6 AIC from SAAM for Giussani Model

	Objective	Scaled Data Variance
s2 : urine	1.955867e+000	4.934547e+005
s1 : WB	7.620755e+000	1.434487e+005

Total objective	9.576623e+000	
AIC	5.746211e+000	
BIC	5.791869e+000	